DESIGN, MANUFACTURING, AND ROUGH TERRAIN ANALYSIS OF A COLLISION RESILIENT FOLDABLE, ADJUSTABLE WHEELED MINIATURE ROBOT: FAWSCY

A THESIS SUBMITTED TO

THE GRADUATE SCHOOL OF ENGINEERING AND SCIENCE

OF BILKENT UNIVERSITY

IN PARTIAL FULFILLMENT OF THE REQUIREMENTS FOR

THE DEGREE OF

MASTER OF SCIENCE

IN

MECHANICAL ENGINEERING

By

Didem Fatma Demir

January 2021

DESIGN, MANUFACTURING, AND ROUGH TERRAIN ANALYSIS OF A COLLISION RESILIENT FOLDABLE, ADJUSTABLE WHEELED MINIATURE ROBOT: FAWSCY

By Didem Fatma Demir

January 2021

We certify that we have read this thesis and that in our opinion it is fully adequate, in scope and in quality, as a thesis for the degree of Master of Science.

Onur Özcan(Advisor)

Yıldıray Yıldız

Özgür Ünver

Approved for the Graduate School of Engineering and Science:

Ezhan Karaşan
Director of the Graduate School

ABSTRACT

DESIGN, MANUFACTURING, AND ROUGH TERRAIN ANALYSIS OF A COLLISION RESILIENT FOLDABLE, ADJUSTABLE WHEELED MINIATURE ROBOT: FAWSCY

Didem Fatma Demir
M.S. in Mechanical Engineering
Advisor: Onur Özcan
January 2021

FAWSCY: Foldable Adjustable Wheeled Stringy Clumsy Robot is a foldable, collision resilient, adjustable wheeled robot which can run through different terrains and inclined surfaces, to inspect areas which are unavailable to humans due to dimensional limitations or hazardousness level; to attend search and rescue missions to cover more area in a shorter duration and to be a part of somatic activities with elders and kids. Hence, it is desired to be non-harmful to itself and its environment in case of any collisions or falls, and persistent on its run under various conditions and terrains as any insect or lizard can.

FAWSCY is an incremental work that till attaining its final version, several legs and wheels; and electronic components and their combinations are investigated. First, c-legs are tested due to its advantages on rough terrains, yet they lack sensor implementation by its constant oscillatory movement. Then ninja stars are tested the robot yet they are so rigid that they sunder from the body in presence of a collision or undesired tracking. Afterwards, the bellow design is modified to be enforced as a wheel and it is the most promising wheel configuration since it can damp all longitudinal, lateral and vertical forces during the impact of a collision and fall. Also, it has appreciable rough terrain performance. However, as well as being soft it is also quite strong that it cannot be controlled for different length configurations for a miniature untethered scale. Therefore, it is not applicable for FAWSCY. On its final adjustable wheel, a novel wicker modular wheel design which exhibits similar behaviour with the bellow design, and its adjusting mechanism are proposed. On the other hand, Raspberry Pi is chosen to be the main processor, and by experiments and investigation through different motors, sensors and control strategies, a two part single board design is

finalized. The body of FAWSCY is also kirigami-inspired and formed by foldable sheets to cover and maintain integrity of its parts and components.

After the design is completed, its performance and capabilities are assessed. First, its indoor run performance, wheel adjustment mechanism, collision resilient properties, obstacle scaling and response to inclination are investigated. The robot is assessed to be suitable for indoor environments, stairs and inclinations without getting disintegrated and harming other living subjects. Then, rough terrain experiments are conducted which resulted in success on grass, gravel and soil terrains with diverse wheel length configurations.

Keywords: origami inspired robotics, foldable robotics, miniature robotics, adjustable wheel, clumsy, threaded, collision resilient, rough terrain, unconventional manufacturing, bioinspried robotics.

ÖZET

ÇARPIŞMA DİRENÇLİ, AYARLANABİLİR TEKERLİ MİNYATÜR ROBOT FAWSCY'NİN TASARIMI, ÜRETİMİ VE ENGEBELİ ARAZİ ANALİZİ

Didem Fatma Demir
Makine Mühendisliği, Yüksek Lisans
Tez Danışmanı: Onur Özcan
Ocak 2021

FAWSCY, katlanabilir, ayarlanabilir tekerli ipli ve sakar bir robot olmakla birlikte, çarpışmaya dirençli, ve farklı engebeli ve eğimli yüzeylerde hareket edebilmektedir. Böylece insan erişiminin zor olduğu ve tehlikeli arazilerin incelenmesinde; daha geniş bir alanı daha kısa sürede taramaya yardımcı olarak arama ve kurtarma çalışmalarında veya yaşlı ve çocukların katılım sağladığı somatik etkinliklere yardımcı olarak katılabilmektedir. Dolayısıyla, FAWSCY'nin herhangi bir böcek ya da kertenkele gibi, kendine ve başkalarına zarar vermeden hareket edebilmesi, çarpışabilmesi, düşebilmesi, farklı yüzeylerde ve koşullarda çalışmaya devam edebilmesi arzulanmıştır.

Son versiyonuna gelene kadar çeşitli tasarım aşamalarından geçen FAWSCY için ilk önce c-bacaklar, farklı yüzeylerde hareket edebilme kabiliyeleri göz önüne alınarak düzenlenmiş ve kullanılmıştır. Ancak, c-bacak ile hareket eden robotun gövdesine sürekli olarak sağladığı osilasyon, üzerine eklenen herhangi bir sensörün çalışmasını zorlaştırdığı için vazgeçilmiştir. 2. kademede ise ninja yıldızları tasarlanıp robota uygulanmıştır. Yuvarlak yapısıyla avantaj sağlarken; sertliği, yıldızın herhangi bir çarpışma ya da istenmeyen yönde maruz kaldığı kuvvet sonucunda robottan ayrılmasına sebep olmakta, böylelikle kullanımını imkansızlaştırmaktadır. O sebeple, yeni bir çözüm bulunmuş ve körük tasarımı bir teker olarak uyarlanmıştır. Bu tasarım, çarpışma ve darbe esnasında üzerine gelen, boyuna, enine ve düşeyine kuvvetleri sönümleyebilmekte böylece FAWSCY için istenen özellikleri karşılayabilmek olmasına rağmen güçlü yapısı teker boyunun ayarlanmasına minyatür ölçülerde izin vermediği için vazgeçilmek zorunda kalınmıştır. FAWSCY'nin son tekeri ise körğk dizaynı ile benzer özellikler gösterebilecek, bununla birlikte daha kolay uzunluk ayarı yapılabilecek, hasır

işlemelerinden esinlenerek yenilikçi bir şekilde tasarlanmış olan tekerdir. Diğer yandan, FAWSCY'nin elekronik parçaları ve tasarımı da aşamalı gerçekleşmiş olup, istenen performansı sağlayan konfigürasyon elde edilene kadar farklı motor, sensör ve kontrol stratejileri uygulanmıştır. Elde edilen devre ise 2 farklı alt sistemden oluşan tek bir devre kartıdır.

Tasarımı ve üretimi tamamlanan robotun, ayrıca performans ve yetkinlikleri de test edilmiştir. Öncelikle iç mekanlardaki çalışması değerlendirilen robot, hareker performası, çarpışma direnci, merdiven inebilme, engel aşabilme, eğimli yüzey tırmanabilme ve teker uzunluğunun değişebilmesi açısından test edilmiş ve yetkinlikle testleri tamamlamıştır. Bununla birlikte engebeli farklı arazilerde de çalışması sağlanan FAWSCY, taşlık, çimlik ve kumluk arazilerde farklı boylardaki tekerleriyle başarı göstererek amacına ulaşmıştır.

Anahtar sözcükler: origamiden esinlenilmiş robotik, katlanabilir robotik, minyatür robotik, ayarlanabilir teker, sakar, ipli, çarpışma dirençli, engebeli arazi, geleneksel olmayan üretim, biyolojik esinli robotik.

Acknowledgement

I would like to express my deepest appreciation to every individual who in a way contributed to this presented work. First and foremost, I would like to thank my academic advisors, Professor Onur Özcan and Professor Yıldıray Yıldız, for providing me this opportunity to do research in the field of my interests. Their guidance, encouragement and visions have become my wisest teachers. Working under their supervision was a great privilege and honour for me.

It was my pleasure to work alongside respected Miniature Robotics Lab and Systems Lab members; Mohammad Askari, Levent Dilaveroğlu, Tamer Taşkıran, Ahmet Furkan Güç, Mert Ali İhsan Kalın, Amirali Abazari, Mustafa Uğur, Shahab Tohidi, Mert Albaba. Yet, I would like to thanks specially Nima Mahkam and Emre Eraslan by being more than colleagues and lab fellow to me. I feel lucky to meet you. Also, Kaan Ekiz and Hakan Malkoç, I want to thank for your contribution to this work and putting your effort more than an undergrad research fellow can.

I also would like to thank my dear BilMech colleagues, Berkay Şahinoğlu, Atakan Atay, Berke Demiralp, Berk Küçükoğlu, Büşra Sarıarslan, Utku Hatipoğlu. I was my pleasure to share the same of working environment by having great memories.

Dear Shari Gamaniel, Mert Yusuf Çam and Aqiq Ishraq, I am thankful for your endless courage, friendship and professional assistance. Also, my precious Ertuğrul Mola, Ayça Deniz Çınar, Serkan Turfan, Müge Uzbilek and Aydan Gülsün who never let me down, see my robot as if their own kid, I am grateful of your presence in my life. These 8 men and women are like a family for me.

Last but not least, my deepest gratefulness is for my family. My love, my home, my inspiration Kaan, thank you for your sincerity, courage and love. My little brother, my play friend, my amusement and annoyment source Yasin, if you

are not around I could not make it. My mom, who always stand as a wall behind me, being a role modal and my dad, making me believe in endless possibles since I was a little kid, thank you for your inspirations and support. Without you, I would not stand as strong as I can today.

Lastly, I want to dedicate this work to my grandma Sebahat Kuzyaka, who left us in sorrow and passed away just before I have finished my thesis. Rest in peace, grandma and say my greetings to my grandfather, Veli Kuzyaka. I always remember you with joy you bring my life.

Contents

List of Figures

List of Tables

Chapter 1

Introduction

1.1 Motivation

When Karel Čapek had come up with the idea of "robot" with his brother Josef Čapek and had finished writing R.U.R.-Russom's Universal Robots(Eng), Rosumaovi Umělí Roboti(Czech)- in 1920, he had the image of humans for his robots. It is still true that robots are designing under the attributions of humans, yet nature provides far more than humans to study on. There are countless animals with different functionality than a human-being offer in mobility, adaptability, resilience, durability, etc. For instance, many insects and lizards are mobile, durable to crashes and falls, resilient to disturbances, and adaptable for variant environments; thus, they have become significant candidates to be imaged for a robot.

Therefore, in this work, attributions of animals are put on the focus of robot mimicking. The main aim is to build a miniature mobile robot, similar to small-sized animals which maintain their functions under persistent and various disturbances, and environments. For instance, during a somatic activity with a child, the robot should run in different playgrounds to accompany the child. The child can hit the robot intentionally or unintentionally, yet the robot should not

harm the child while keeping its integration and functionality. Hence, to achieve these somatic activities, search and rescue missions, surveillance operations, or hazardous environment explorations, a manoeuvrable, compliant, adaptable, and resilient robot that can run different terrains is needed.

1.2 Miniature Mobile Robotics Literature

Miniature mobile robots provide a significant contribution on several tasks such as inspection and exploration on hazardous and obscure areas, surveillance, search and rescue(SAR) missions, educational and/or social assistance for kids and elders; as they are small, silently operated, highly manoeuvrable, lightweight, relatively cheap and do not harm other beings -animals, plants or human beings- in case of collision. However, designing and building a miniature robot has challenges in manufacturing, actuation, control, and retrievability; as in miniature scales, effective forces and strength of materials differ, and available volume for components and mechanisms is limited. Thus, unconventional thinking and manufacturing techniques become a requirement to develop mobile miniature robots.

One of the early unconventional manufacturing techniques is SCM - Smart Composite Microstructure fabrication developed in UC Berkeley [2] for millirobotics. The technique is consisted of developing composite and laser beams to cut. By the time, it is enhanced by layering different materials on top of each other and then adapted to mobile robotics [3], there are exhibited successful robots such as RoACH [4], and DASH [5]. Later, [6] forms the SCM to develop self-folding limb and robot with the aid of shape memory composites. Availability of laser cutting and creating folding patterns infused the well-known old arts Origami and Kirigami more into robotics. Rather than being an inspiration for mechanisms, the robots are designed directly as origami or kirigami objects as a whole, or their bodies and limbs are designed as separate origami/kirigami objects and assembled together. While [7] and [8] explains general rues and mathematical patterns, wormlike robots [9], quadrupeds such as MiniAQ and CQuad [1,10,11],

modular robots such as SMolBot [12] and hexapods, octopods, and gripper mechanisms [13] are designed and manufactured from different paper-like single sheet materials and silicon [14]. On the other side, SCM and Kirigami are implemented on MEMS processed to exhibit milli-scale full functional mobile and/or flying robots where the limbs or whole robotic structure designed as different layers including circuitry elements as SMA (Shape Memory Alloys) or PTZ (piezoelectric materials) are cut separately and then aligned and released to robots [15]. Some triumphant examples of MEMS are as follows: HAMR, which is manufactured by PC-MEMS [16, 17] and Flying Monkey with pop-up CAD [18].

There exist unconventional and non-origami-inspired manufacturing methods as well, as 3D- printing [19, 20] and PDMS molding [21] to design fully functional mobile robots. The other manufacturing methods used not mobile robots yet inspire mobile robotics are IFI (Inverse-Flow-Injection) and DCR(Deep-Cure-Repeat) [22] to manufacture manipulative properties and SDM - Shape Deposition Manufacturing to obtain built-in multi-material characteristics for desired parts of the robot [23, 24].

The other challenge for a mobile robot that is significant as manufacturing is the environmental impact. Any non-smooth environment may limit the functionality of a miniature mobile robot. Thus, collision-resilience and adaptability to different terrains are also desired features for a mobile robot. Although it is discussed in Section 2.2.1 in detail, RHex [25] exhibiting rough-terrain obstacle-crossing and [26] implementing embedded dampers to over-come the impact of a crash are two tasty examples to introduce.

1.3 Research Aims and Contributions

By FAWSCY aka **Foldable Adjustable Wheeled Stringy Clumsy** robot, it is desired to build a miniature robot that is lightweight, less equipped possible but maximized performance. Additionally, by manufacturing techniques and chosen materials, it can exhibit collision resilience characteristics that cannot

be damaged or cannot damage the collided object. It is an essential feature as running indoor and outdoor, many robots can interact with children and elders, and various animals, i.e., cats, dogs, birds, lizards, etc., and even some herbs as flowers, trees; and any-side of this interaction should not be harmed. A way to achieve it to make the robot collision-free by equipping it with many sensors to allocate any organic or non-organic objects and calculate expected collisions and avoid them. This approach requires many processors, sensors, drivers, and bulky power resources to maintain sensing and drive, which transforms the robot either a tethered robot and/or becomes a metric scale robot with hard materials such as steel and aluminium, and quite heavy. Thus, if it fails to predict and avoid collisions, it harms the object of collision and possibly itself, as well. Then, another solution arises as building an untethered and resilient robot. Therefore, during the design and test phases, without bulky and numerous electrical components, connection, and carrier parts, minimization of equipments and unconventional production methods are investigated. Also, materials lifetimes are considered. It is desired to be readily producible and cheap, so during or after the mission, it can be disposable and re-buildable in case of need.

Hence, FAWSCY contributes to the miniature robotics literature by providing an adjustable wheel in length and implemented into a robot to increase terrains it can run through. Opposing the similar examples in literature, FAWSCY can run various environments by differentiating its wheel length when necessary. Moreover, it can climb over inclinations and across obstacles. Another distinguishable feature of FAWSCY is that it can interact with living things; for instance, if a collision happens with humans and animals, it continues its task without harming or being harmed.

1.4 Structure of The Thesis

The work done in this thesis is compiled in the manner expressed as follows.

Chapter 2: Evolution of FAWSCY focuses on literature reviews about

miniature mobile robotics and initial versions of FAWSCY to attain desired research aims and objectives. It introduces various leg and wheel designs, electronic schemes, and initial tests.

Chapter 3: Design and Manufacturing of FAWSCY explains the final version of robot. It provides detailed information of wheel and body design and manufacturing steps. It also talks about its PCB and control architecture.

Chapter 4: Tests and Evaluations of FAWSCY introduces the resilience and performance evaluations of robot. Its running performance on several terrains, interactions with obstacles and climbing on inclined surfaces are studied. Finally, the effects of fall on the robot and the effect of wheel characteristics on the robot is analysed.

Chapter 5: Conclusion and Future Work sums up the work and glimpses what can be enhanced and advanced.

Chapter 2

Evolution of FAWSCY

In the light of Motivation presented in Section 1.1 and to meet requirements highlighted in Section 1.3, FAWSCY has passed many stages and evolved to its final form being an $12cm$ length, $6cm$ height, $18 - 25cm$ width and $272gr$ robot, exhibited in Figure 2.1. Therefore, in this chapter, its design evolution is discussed as material selection, different leg designs, body modifications and its circuitry.

Figure 2.1: Final version of FAWSCY

2.1 Material Selection

In theory, to form an origami and krigami art piece, any paper would work. Yet, the paper should hold the creases. It means that it should not back-lash or wear out. Thus, when choosing a paper for an origami design, those properties of the paper should be considered: thickness, strength, crispness and forgiveness [27]. Moreover, in this work, the origami piece is created to build a miniature mobile robot, which means that the chosen origami paper is used as the primary material for its body and limbs. Thus, the selected paper's dynamical and kinematic properties are also important to prevent the robot from any form of failure, i.e., fatigue cracks, tearing, perforation. Another aspect of selection is resist-ability to water, heat, etc., to keep the integrity of the robot. In the sense, PET: polyethylene terephthalate, sheets and Kapton® sheets are favourable candidates. PET and Kapton® are both durable, easy to process under laser cut without harmed,

waterproof, transparent and available in different sizes and thicknesses. It is observed through experiments that thinner PET and Kapton® sheets exhibit more elastic properties while they hold creases better, yet PETs are folded effortless than Kapton®. On the other hand, Kapton® has higher fatigue-resistant and insulator properties [28].

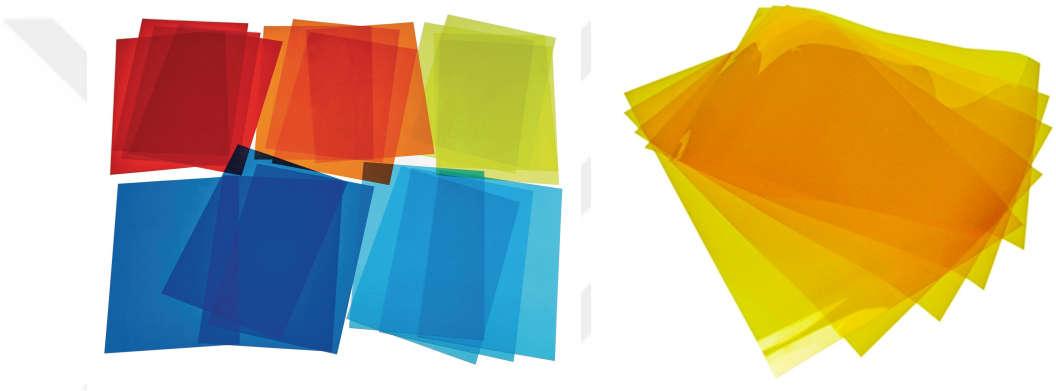

(a) (b)

Figure 2.2: (a) 100 μm thick PET steets, (b) 100 μm thick Kapton® sheets

2.2 Legs and Wheels

2.2.1 Literature Review

To overcome environmental impacts on a miniature robot, how to activate its motion is crucial as not only the transportation of the robot itself by running, crawling, jumping, or flying but also achieving the desired path and without failure of the robot are required. Thus, the design of limbs plays a prominent role.

Mobile robots mostly use legs or wheel-like structures, and in some cases, combination or transition of two. RHex [25] and MutBug [29] are hexapods with

4-bar mechanisms inspired by cockroach to run over rough terrain. Quaid [1], SQuad [21] and Quattroped [30] are semi-circular hooke-like designs for obstacle climbing. Wheel-like origami-inspired and composite designs are mostly adequate to past through narrow or short slits by changing diameter of wheel or length of wheel [31–36]. Moreover, [30] and [33] transit their wheels to legs or vice versa to benefit both designs advantages'.

There are also extra-ordinary examples of wheel and leg designs that focus on joints, extra features or ideas differently bio-mimicked and origami-inspired mechanisms. For instance, Genbu [37], and Mini Rover [38] wheeled robots where their joints allow wheels to rotate and bend on different axes than the drive axis, which makes them favourable for extremely rough-terrains. On the other hand, adding different features like paddles and grousers enable robots to investigate hazardous environments [39, 40].

2.2.2 C-Leg

For FAWSCY's collision resilience properties, the first proposed solution was C-leg designs that our lab members have already designed and used [1]. It is light-weight, foldable, springy to handle collisions and has enough strength to carry the body load. In Figure 2.3, its design procedure is presented. Standard c-legs that are basically semi-circles, this version of C-leg differently, is fitted into a center that is the pivot point for motor connection, and c-shape is deformed to maintain a constant height for the body [1]. By its existed advantages, the design is ready to implement yet; it's needed to be scaled up to our body dimensions. In Figure 2.3, it is scaled version and implementation is also presented.

(a)

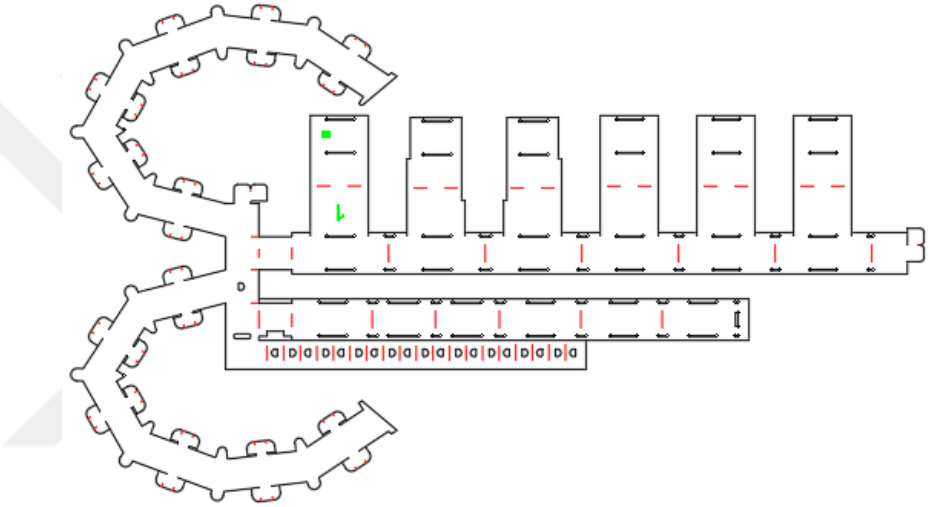

(b)

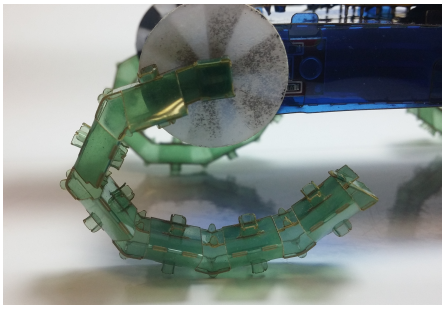

(c)

(d)

Figure 2.3: (a) Deflected C Formation of leg [1], (b) C-leg Autocad Desing, where black solid lines are cut, red dashed lines are crease references. C-shapes are the skeleton and the extensions with rectangles are triangular closets of leg to form its 3D shape. D-centered squares form the motor hub, (c) Original sized c-leg implemented on CSuad [1], x2 scaled c-leg implemented on first version of the robot (d) .

Through the experiments, it is observed that, despite its advantages, due to the incomplete circularity of legs' design, the body always touches the floor in a sinusoidal fashion. In small-scales and with less-sensor, it does not affect the performance of the robot significantly. Yet as the body enlarges and gets heavy, impact forces on the body increase, and the robot's life-cycle is shortened. Also, those impacts cause noise on the sensor outputs, as it can be seen in Figure 2.4. Another problem encountered on the run of FAWSCY with c-legs is unpredictable detachment of the legs. To prevent detachment issue, motor caps are design (Figure 2.5), yet problem is persistent. Thus, the implementation of c-legs is inapplicable.

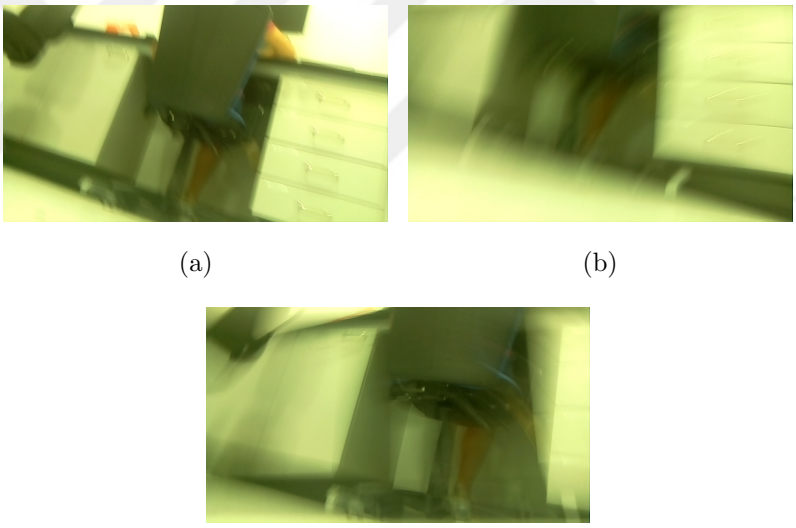

(a) (b)

(c)

Figure 2.4: Pi Camera recordings while running with c-legs. Due to its continuous oscillatory body movement, images blurred that objects and edges cannot be distinguishable.

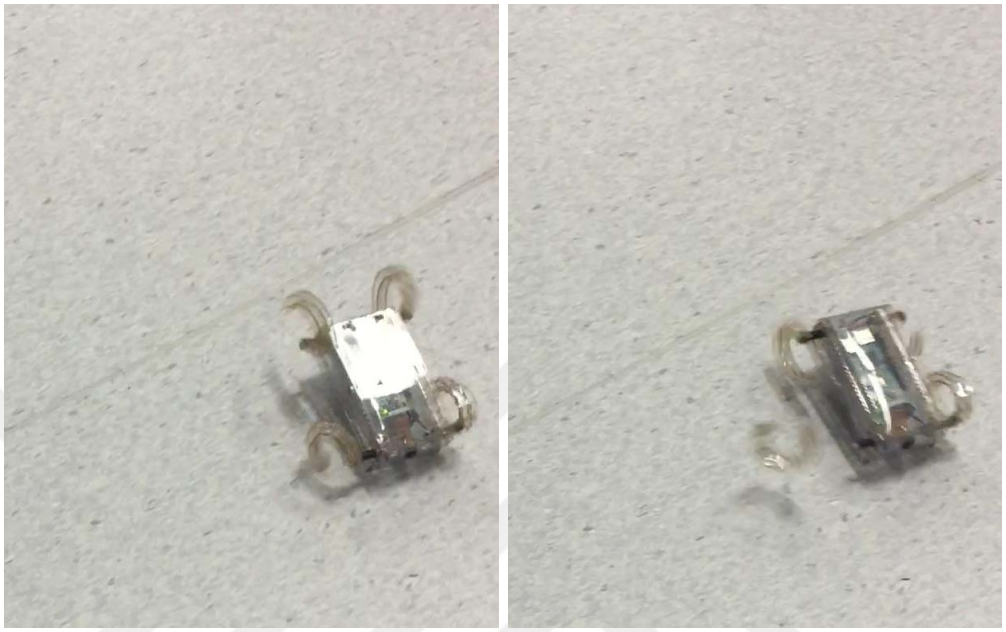

(a) (b)

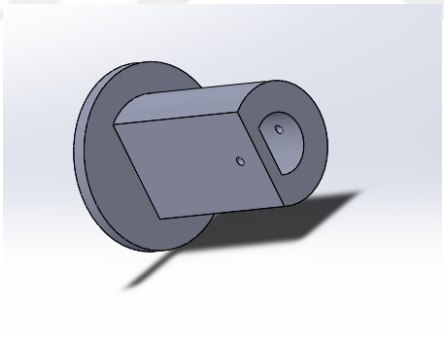

(c)

Figure 2.5: (a) - (b) C-Leg detachment (c) Designed C-leg motor caps to prevent leg detachment, drilled with motor and pinned.

2.2.3 NinjaStar

After the inapplicability of C-leg, a design which has both circular conformity and spiky features is sought. While circular conformity eases sensor implementation, as it can be seen in Figure 2.6, and body protection, spiky features hooke the obstacle as the C-leg does. Even though there are origami wheels in the literature

as presented in 2.2.1, none of the examples give the desired duality. However, traditional origami samples do provide circular spiky shapes as ninja star [41].

(a) (b)

Figure 2.6: Pi Camera recordings while running with ninja stars. Due to motion, there exist minor motion blur on images, yet features and edges are distinguishable.

The ninja star is a modular origami diagram consisted of 8 identical elements. For the wheel application, it is also added a motor mounting element, and its element design is also modified to confirm the integrity of the structure. Figure 2.7 represents the design where red dash lines indicate crease reference lines and continuous blue lines are the cut lines and geometries. White lines are design reference lines for assembly dimensioning. Each element has a square base where the upper and lower triangles and lower vertical lines are to transform the base into a parallelogram. Slots are housings for the next-element edge, which are folded inside by corners. Circles are motor-housing's assembly holes which are pinned by rivets. Motor housing consists of rivet assembly holes on the tangents of its centre circle, and on the center, tightly dimensioned D-shaped motor housing based on the dimensions of the motor shaft.

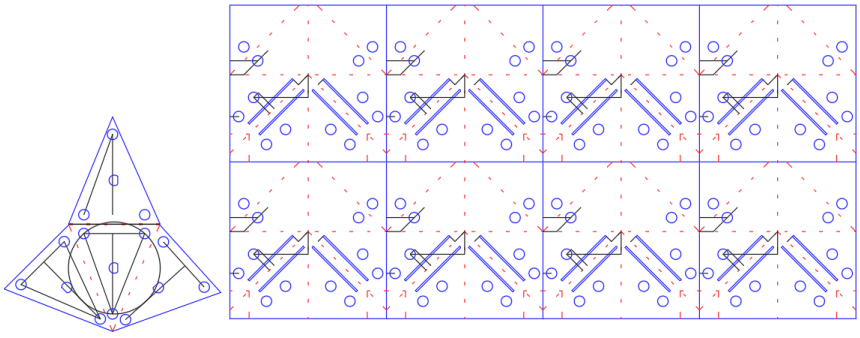

(a)

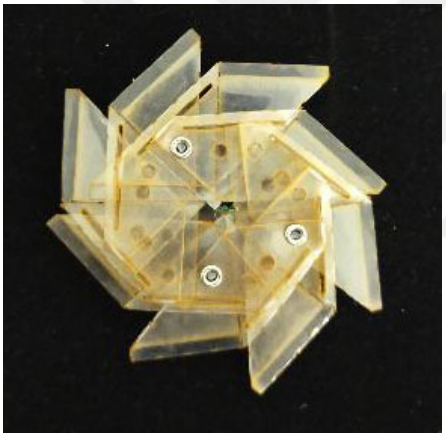

(b)

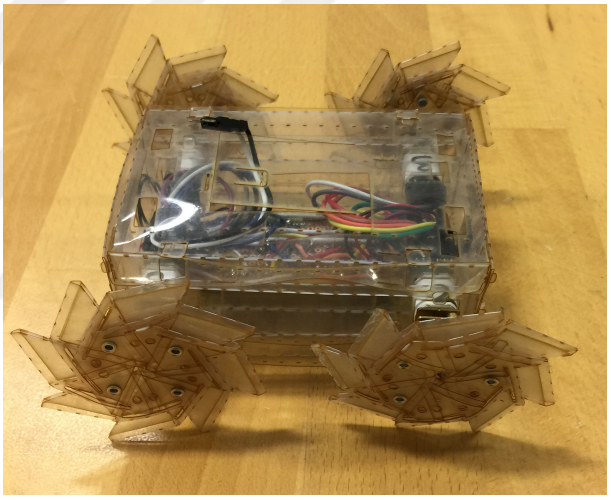

(c)

Figure 2.7: (a) Ninja-Star Autocad Desing, (b) Folded and assemblied Ninja-Star from PET sheets, (c) Ninja-Stars assembled to robot.

Although the ninja star exhibits desired features, it also has some problems. During the assembly, tight-fit D-shape housing goes under pre-stress. Also, the assembled ninja star has higher stiffness than C-legs such that when the robot collides with objects, it does not perform any backlashes as C-leg does. Thus, the collision force is directly transmitted to motors and the body and contributes to 4-layered motor housing's initial deformation. In case of collisions, those deformation causes wheels to detach from the motors (Figure 2.8) which violates the robot uniformity as well as collision-resilient feature of FAWSCY. Moreover, motor housing deformations result in alignment issues as Figure 2.9 displays. As the

ninja-star's stiffness decreases the contact area with the ground, which prevents compensation of misalignments, thus the performance of the robot also decreases. Therefore, ninja-star becomes a less favourable candidate as a wheel.

Figure 2.8: After a few runs, due to wear-out it detaches its wheels.

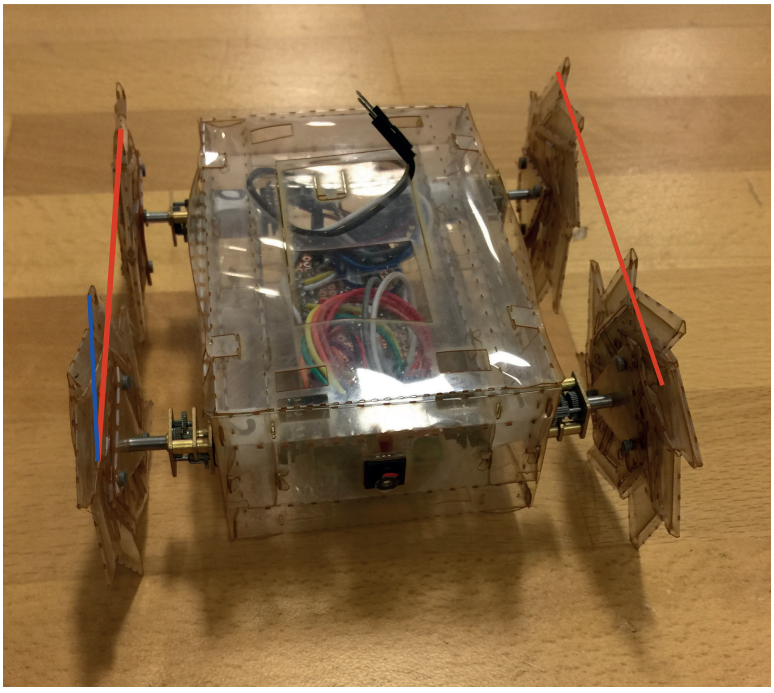

Figure 2.9: Misalignment of ninja star wheels are marked as red lines, reference and blue lines distortion. During the runs, presented distortions propagate and lead to either detachment of the wheel or malfunction of robot.

2.2.4 Bellow

After ninja star and c-leg failed, [42] inspired a different type of wheel that can deform by itself and behave as Genbu does [37], but it is counting on its geometrical shape and material rather than its joints. Then, it is found that the Kresling structure is used for different applications, i.e. worm-robotics [9, 42], medical applications [20, 43, 44]. Kidambi and Wang analyse torsional and longitudinal properties of the structure [45] that it can bend, rotate, handle thrust by changing its length and damp perturbations. Moreover, it is a controllable-edgy structure. Hence, it is a strong candidate as a wheel for a collision-resilient origami-inspired robot. Additionally, its length-adjustable characteristics increase its manoeuvrability.

2.2.4.1 Design

The structure is composed by Butler's [44] Kresling Units' formulations in Figure 2.10. Wheel outer diameter, D is calculated by FAWSCY's body dimensions. It is desired that, body is not touching the ground on operation, and body, hence the wheels should be symmetric in case the robot flips its top to bottom after falls and/or interaction with obstacles, so that it can still perform. Then, the Kresling units are calculated by eqns 2.1, 2.2 and 2.3 to form the final design.

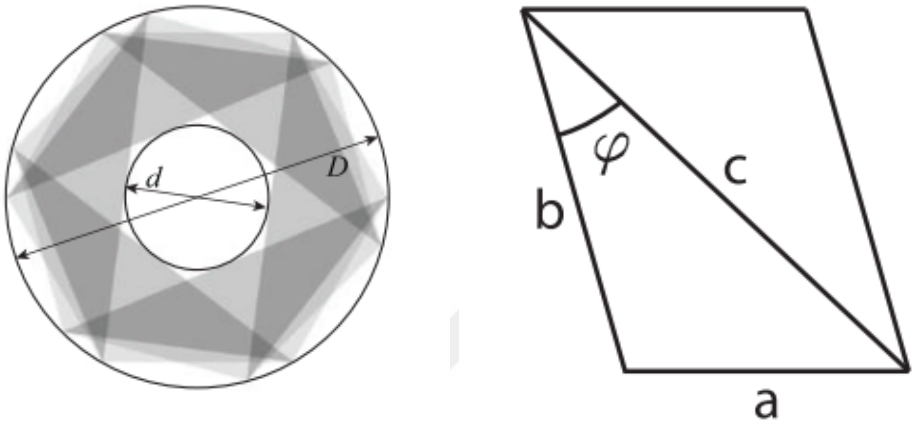

(a) (b)

Figure 2.10: (a) Bellow diameter representation, (b) Kresling unit parameters

$$a = D \sin \frac{\pi}{n} \tag{2.1}$$

$$b = D \sin \left(\arccos(\frac{d}{D}) - \frac{\pi}{n} \right) \tag{2.2}$$

$$c = D \sin \left(\arcsin(\frac{b}{D}) + \frac{\pi}{n} \right) \tag{2.3}$$

Figure 2.11 explains the 2D scheme of the bellow wheel. The design is cut from both PET sheets and Kapton® as it can be seen in Figure 2.13, and it is observed that Kapton® outperforms. Also, as discussed in Section 2.1, Kapton® has better strain properties and a longer life cycle than PET sheets is a better solution for the bellow wheel. Thus, in Figure 2.12, production of layered Kapton® sheets are presented.

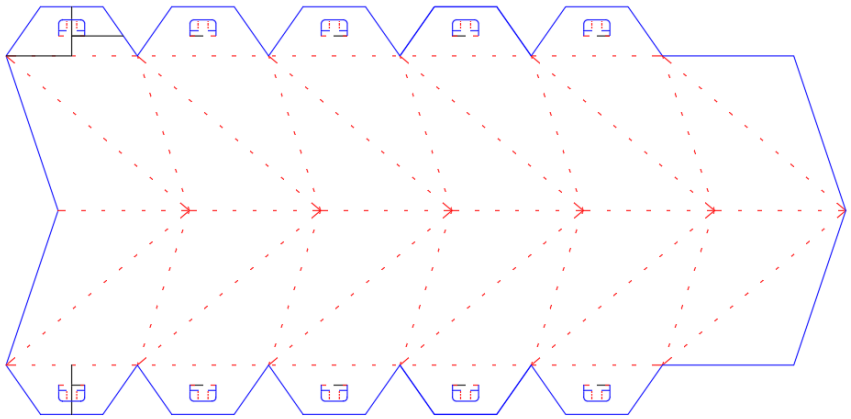

Figure 2.11: Bellow autocad design, consisted of 12 Kresling units. 5 unit at the bottom and the 5 unit at the top form the wheel. Trapezoids extented from those units are connection-sites to the hubs b u-folds. 6th Kresling units exist to finalise cylinder shape as 6ths adhere to 1sts. Blue continous lines represent full-cuts while red dash-lines represent crease references, dash-cut by laser cutter.

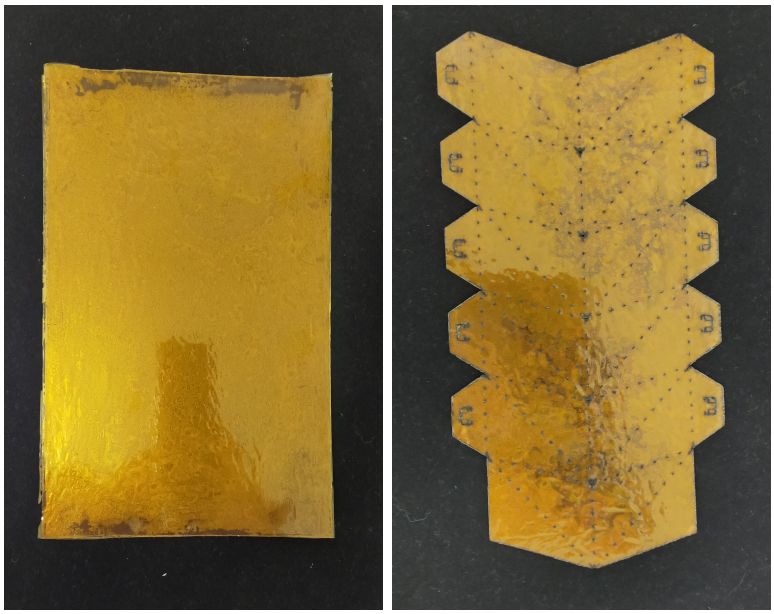

(a) (b)

Figure 2.12: (a) 3 Layers of Kapton®, produced as 1 layer of Kapton® (K), 1 layer of Adhesive film (A), 1K, 1A, 1K on hot plate at 195 °C for 30 mins. (b) Autocad design is cutted on the 3-layered-Kapton® sheet.

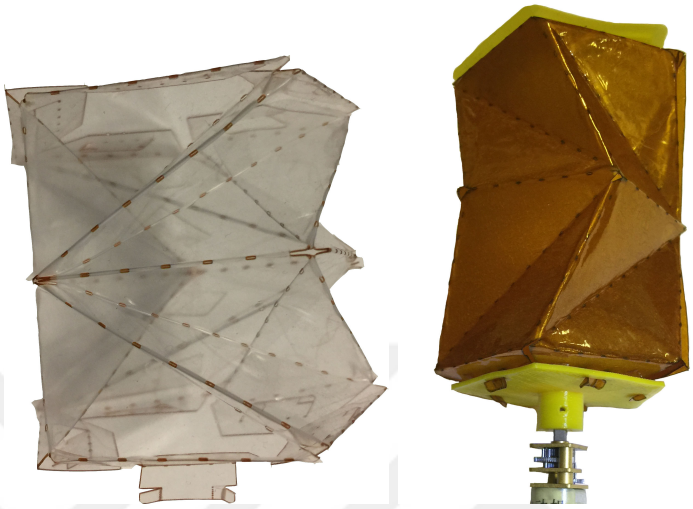

(a) (b)

Figure 2.13: Bellow design cutted and folded from (a) PET , (b) Kapton. As it can be seen, PET sheet has sharp cuts which propagates as fracture under longitudinal and lateral stress whereas, Kapton sheet preserves its material integrity. Hence, Kapton Bellow wheel survives for longer duration.

Finally, Figure 2.14 shows the hub and lids to enclose the bellow and motor camshaft to connect wheels to the robot body. Hub and lid have a smaller outer circle diameter for the pentagon than D (Figure 2.10) to ensure that the robot runs on the wheels, not on the hubs and lids. Both hubs and lids are 3D-printed from a flexible material, TPU, that conforms to the elasticity of Kapton® and the design and slots for where u-folds lock. Hub has a motor mounting cylinder that suctioned the TPU over PLA camShaft, preventing detachment of the wheels from the robots contrarily to c-leg and ninja star.

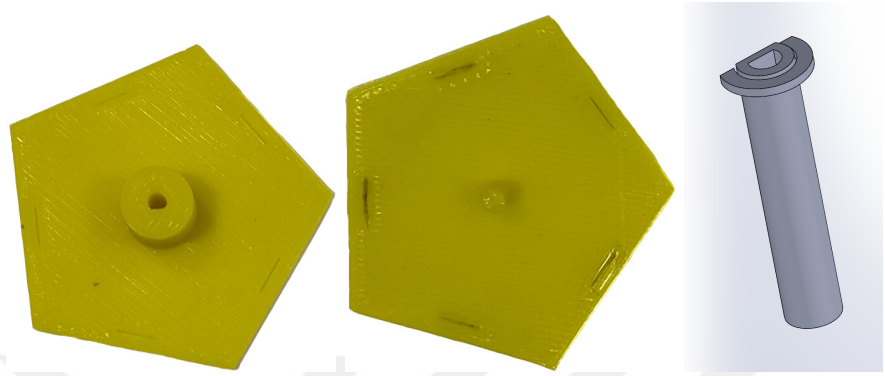

(a) (b) (c)

Figure 2.14: (a) Bellow Hub to mount the motor and connect wheel to the robot. (b) Bellow Lid. (c) Motor Cam Shaft

2.2.4.2 Implementation of Bellow Wheel

The cut and folded bellow wheels are assembled to the body as Figure 2.15 shows. However, Kapton® surfaces are quite smooth and slippery, and on operation, wheels are sometimes skidding and cannot climb inclined surfaces. Figure 2.16 and 2.17 explain observed skid and fall-out behaviours respectively, by consecutive time shots of experiments.

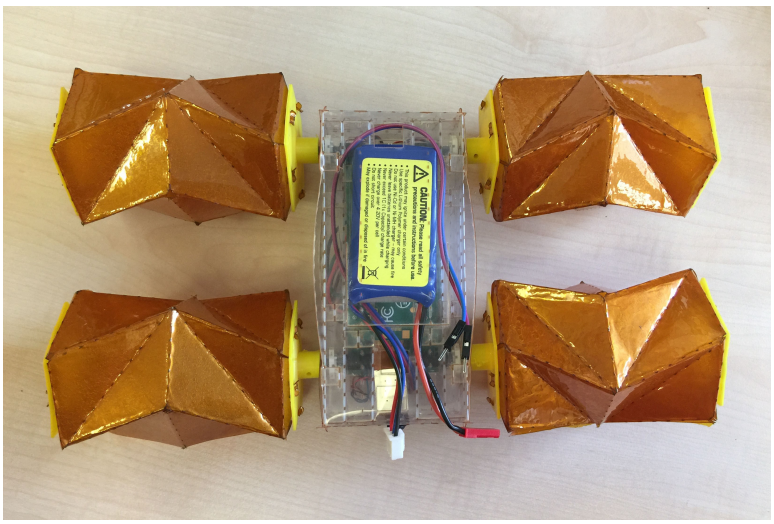

Figure 2.15: Bellow-Wheeled Robot

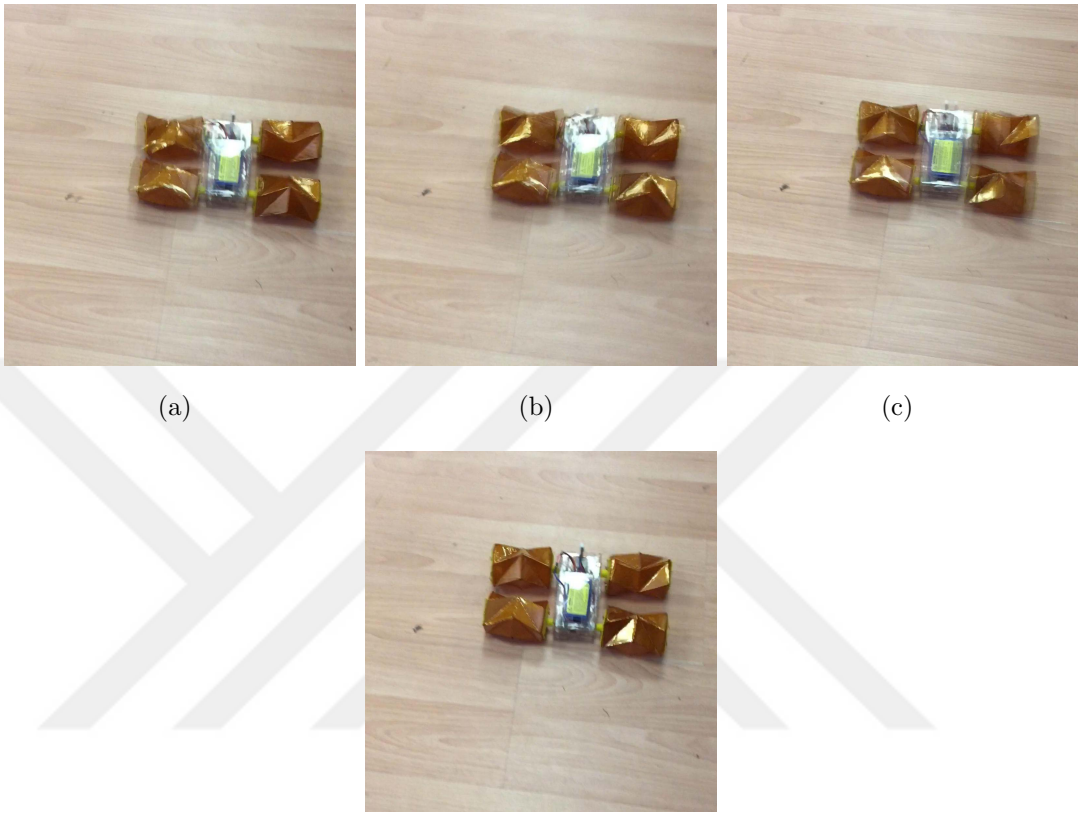

(a) (b) (c)

(d)

Figure 2.16: Skid failure of bellow wheel.

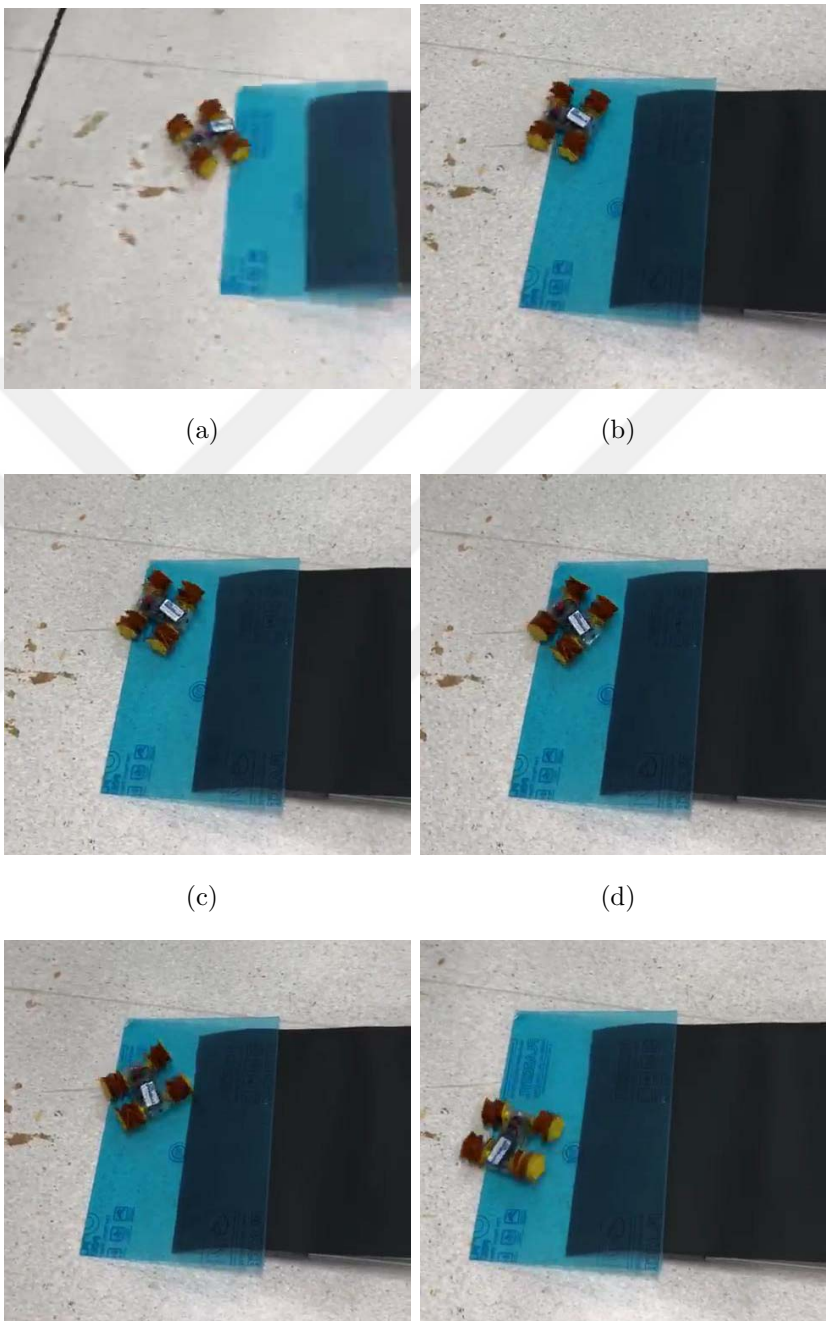

(a) (b)

(c) (d)

(e) (f)

Figure 2.17: Inclined surface climbing Failure of bellow wheel.As it can't climb up, it steers right or left then falls from the inclination.

2.2.4.3 PDMS Coating

The bellow wheels' glassy surface causes a temporary skid of the robot on flat surfaces and prevents the robot from performing on inclined surfaces and obstacles encounters. Therefore, the need for increasing friction between the ground and the wheel has appeared. By the time, our lab members are using Polydimethylsiloxane (PDMS) in different ratios to fabricate legs and bodies [12, 21], and PDMS coating is observed as a solution. Then, a specific procedure is adopted, as the PDMS ratio and its curing agent, and curing time and curing temperature affect the characteristics of the output PDMS material. Also, as there exist four different wheels, coating for each should be identical to have the identical friction forces on each wheel to maintain a straight trajectory and decrease the load on the control function. Therefore, the adopted procedure and the mold to maintain the wheels' uniformity are presented in Figure 2.18.

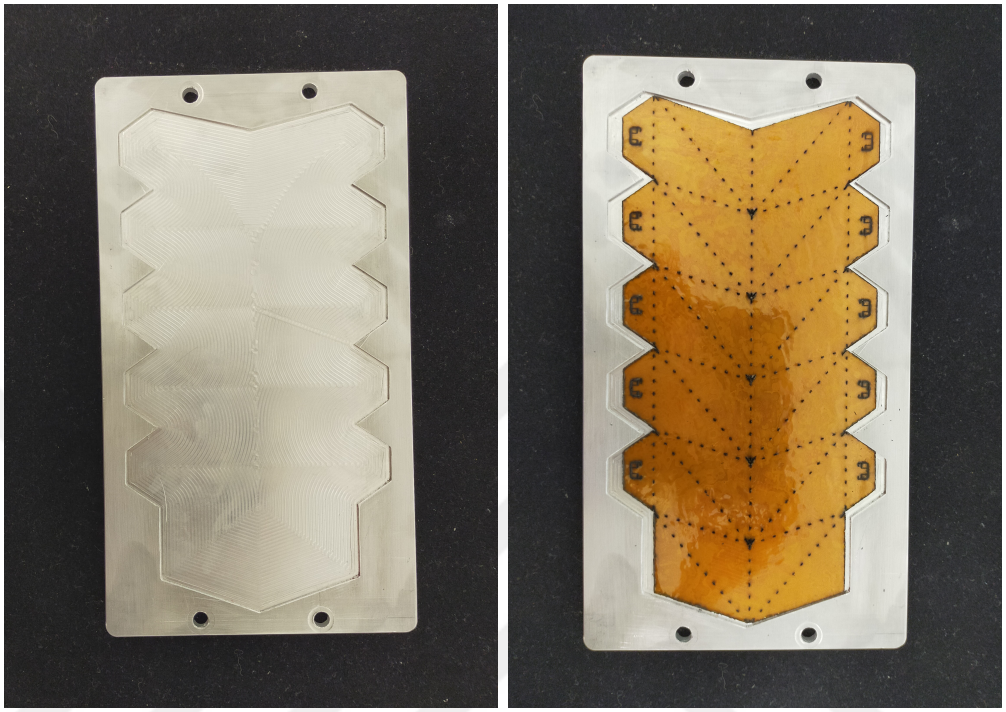

(a) (b)

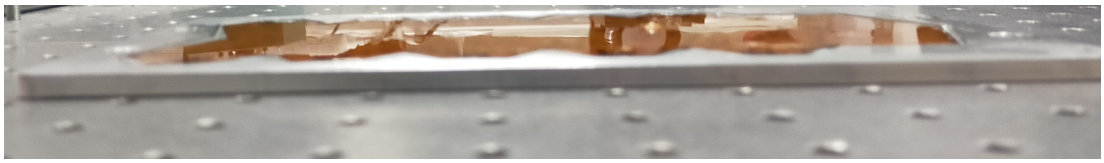

(c)

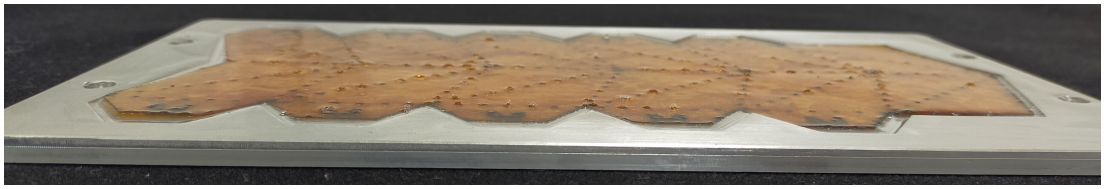

(d)

Figure 2.18: (a) Milled aluminium mold. (b) Cutted Kapton® (in Figure 2.12) is placed on the mold. (c) By 10:1 ratio of PDMS and its curing agent, respectively are mixed and poured on the sheet. (d) The poured-plate is placed on incubator at 80 °C for 50 mins to be cured.

2.2.4.4 Tests and Results

By the PDMS coating on bellows, performance of the robot is increased and clumsiness tests are conducted, i.e. obstacle climbing, stair-like surface climbing, inclined surface climbing and fall-off the robot from certain heights. Moreover, as bellow design allows different wheel lengths, each test is repeated on 3-different wheel length: 7 cm - full length, 4.5 cm - middle length and 1.5 cm - minimum length, which are visible in Figure 2.19. Table 2.1 and 2.2 exhibit qualitative results of the tests and Figures 2.20, 2.21, 2.22 and 2.23 visualise test set-ups and their results.

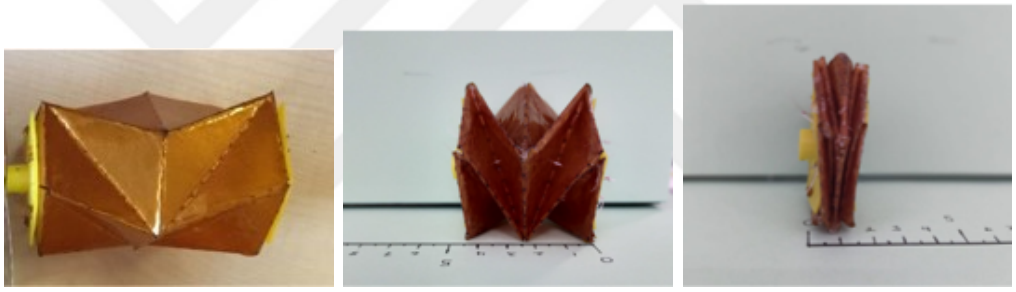

(a) (b) (c)

Figure 2.19: (a) 7 cm full length bellow wheel (b) 4.5 cm middle length bellow wheel (c) 1.5 cm middle length bellow wheel

Table 2.1: Achievable test limits for Bellow wheel length configurations

Operation	1.5 cm	4.5 cm	7 cm
Obstacle Scaling	2 cm	1.6 cm	2 cm
Inclined Surface	11	6	15
Fall	40 cm	40 cm	40 cm

Table 2.2: Achievable narrowest and highest obstacle scaling limits for stair-like case where l:staircase height, t: staircase width, h: stair-rise, including maximised and minimised Bellow wheel length configurations

Wheel Length	l	t	h
1.5 cm	0.5 cm	1 cm	3 cm
7 cm	0.5 cm	1 cm	3 cm

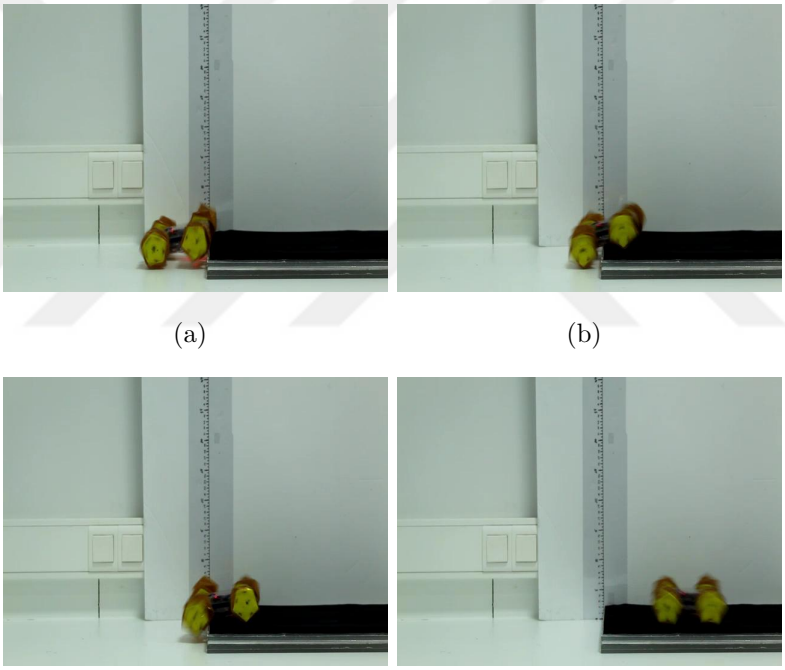

(a) (b)

(c) (d)

Figure 2.20: Obstacle scaling of height 2 cm, experiments of bellow with maximised length configuration.

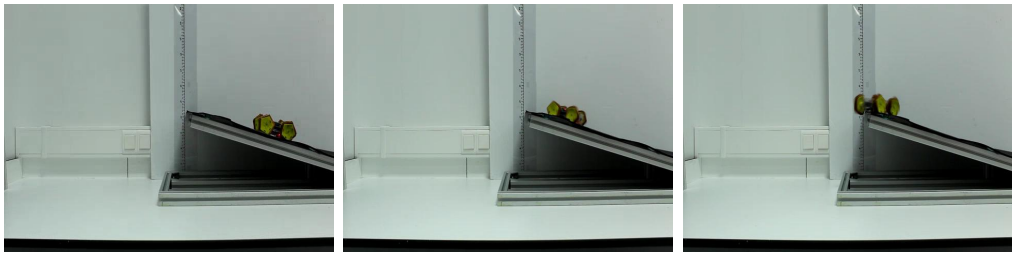

(a) (b) (c)

Figure 2.21: Inclined surface climbing with inclination rate of 11° of bellow wheel with minimum sized length configuration.

(a) (b) (c)

(d) (e) (f)

Figure 2.22: Fall experiment of bellow wheeled robot. It successfully maintains its run after falling 40cm of height.

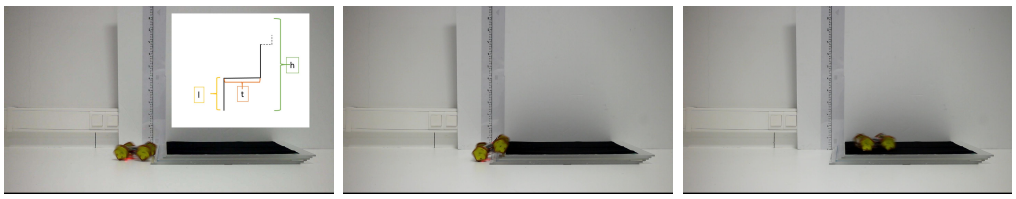

(a) (b) (c)

Figure 2.23: Stairlike obstacle scaling of bellow wheel where l:staircase height, t: staircase width, h: stair-rise and presented on northwest of (a).

After promising test results, a mechanism to change wheel length is designed (is discussed in Section 3.2). However, changing four bellow wheel lengths requires torque beyond the torque supply of any stepper motor that can fit onto our system's dimensional limits. The layer count of the Kapton® sheets, PDMS coating, and design parameters affect the torque requirement. Any increase in these strengthens the wheel more and increases the required torque to pull. Hence, the implementation of the bellow wheel fails. A new wheel, discussed in Section 3.1, is designed.

2.3 Body

As the robot is an origami-inspired lightweight robot, its legs and wheels and its body are designed as a kirigami structure and PET sheets are used. By various leg, wheels, and circuitry elements, the body creases are transformed, yet its structural elements, i.e., T-folds (in Figure 2.24.a) for columns and rigidity, U-folds (in Figure 2.24.b) to hold in place T-folds and shutters, are essential and remained unchanged. Rather, their dimensional variations and functionality are played. Then, as consistent with the wheel designs, in the following body AutoCad designs, the solid blue lines are cut lines and dashed lines are crease references. The body has one or two consecutive T-Fold creases on the sides to frame the body or place equipments, i.e., motors and sensors. It has many slots to place U-folds, and inner rectangles to be cut on layers or T-folds to convey the

wiring throughout layers.

Figure 2.24: (a) T-fold as a beam of body (b) U-folds as lock mechanism of structures

The first body is designed for c-leg. In run with c-legs, the body is always in contact with the ground from either front or rear in a sinusoidal fashion. Moreover, c-leg can run the robot regardless of which side is on the top or bottom. Therefore, the body is created as 3 layers; in the middle layer is where the circuit is placed, the bottom layer is battery holder and semi-damper, and finally, the top bottom is free layer so that it is symmetric by motor axis, and extra top and bottom layer would decrease the impact on the body. Hence, the body in Figure 2.25 is formed and folded.

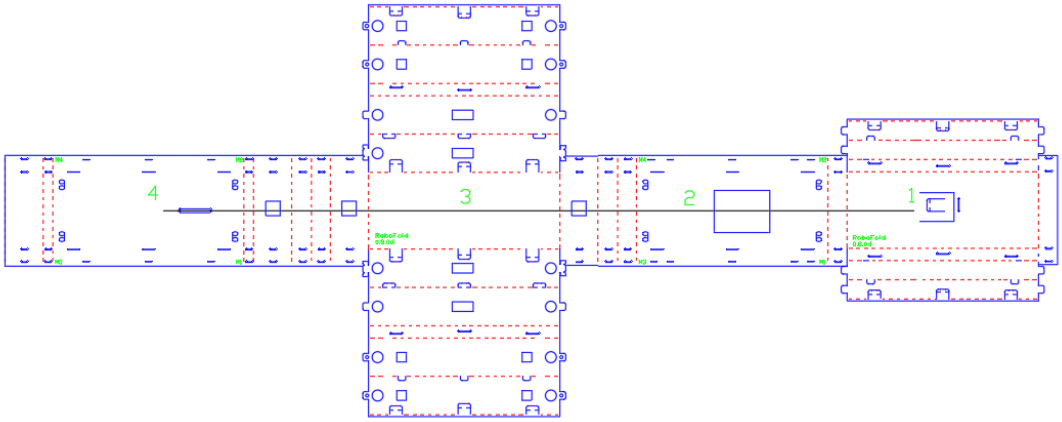

Figure 2.25: Autocad design

However, c-legs are proven that it is not applicable. During the time being, there are modifications on circuitry elements, as well. Hence the body is changed to be compatible with ninja star wheel and updated PCB and demonstrated in Figure 2.26. As pointed out before, the design principles are remained yet, the shape of motor holder is transformed from circle to rectangle to hold the motor in place, and dimensions are updated. The 3-layer structure and its symmetry are preserved.

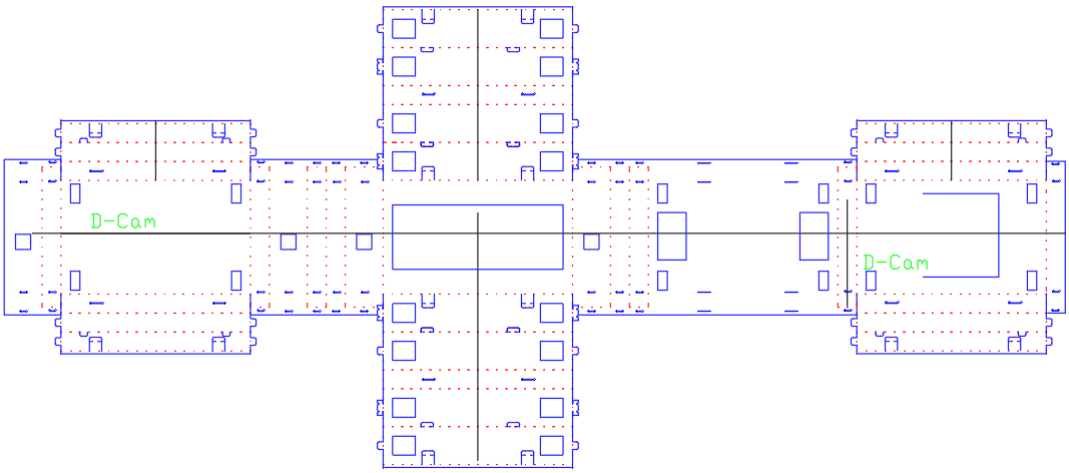

(a)

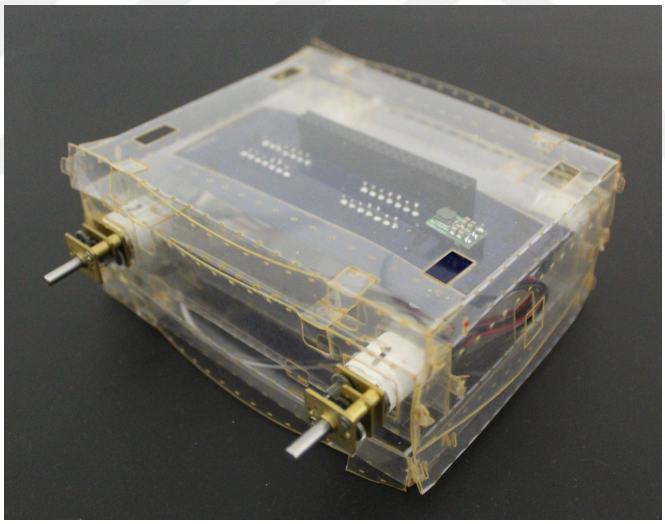

(b)

Figure 2.26: (a) Autocad design (b) Implemented body

Through the experiments, it is observed that raspberry pi is not an efficient way to control 4 motors separately (it is discussed in Section 2.4), so that an Arduino circuit as low-level controller is coupled with pi, and also wheels are switched from ninja star to bellow, thus the body is transformed. 3-layer design is also preserved with its symmetry yet differently, for this one, several rooms for varied circuitry are needed. Battery resides on one layer, Arduino pcb occupies the middle and raspberry pi is on the remaining layer. Thus, first, middle layer is formed by 3

T-folds to hold in place both motors and rotary sensors. However, on the run, T-folds are insufficient to maintain parts aligned which leads malfunction of robot. Then, a rigid motor-casing where 2 motors and rotary sensors are mounted back to back, is used. Figure 2.27 expresses the versions of the body and motor casing.

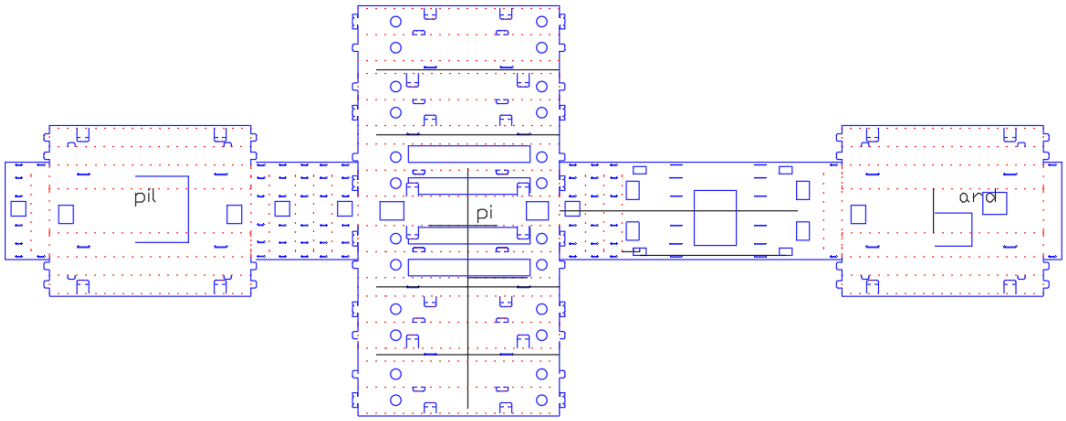

(a)

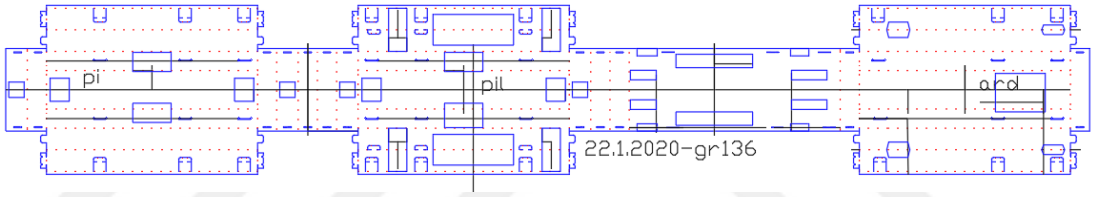

(b)

(c)

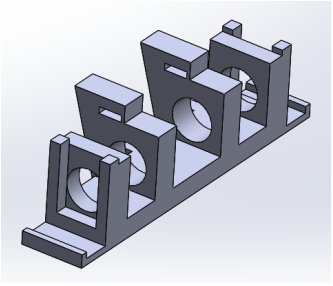

(d)

Figure 2.27: (a) AutoCad design of the first version without motor casing (b) AutoCad design of the second version with motor casing, (Implemented body (d) Motor casing: PLA 3D-printed)

2.4 Circuitry and PCB

2.4.1 Electronics Selection

In order to achieve aims and objectives presented in Section 1.3, FAWSCY is equipped by 4 dc-motors which are driven individually to increase manoeuvrability. Hence, to run the robot in a controlled fashion, each motor is coupled with a sensor that measures and feeds the running motors' velocity. It is also added a camera to use image feedback as if the desired task is achieved or else to confirm the subject of search or mission is detected. This subject can be a life in distress or imminent danger, or the child or elder to be accompanied for care or play, or an object in an investigation medium. Thus, there is a need for a processor which have the computational capacity to process incoming visual data. Additionally, there are limitations on electronics regarding mechanical design, such as it is a miniature robot that the working range is in centimetres or there is a weight limit that foldable designs would carry. Therefore, the electronic components chosen should satisfy the needs and limitations simultaneously.

In the light of constraints, Raspberry Pi Zero W is chosen as the main processor. It is small, lightweight and has accessible 26 GPIO pins and a built-in camera connection and protocol. It also connects Wi-Fi, which enables remote control or instant manipulation of the robot by the operator. As a camera, Raspberry Pi Zero Camera is selected due to both compatibility with pi and its remarkable small size ($1cm^2$). For motors and sensors, initially, Pololu's DC motors (136:1 Sub-Micro Plastic Planetary Gearmotor) and QTR-1A Reflectance Sensors are chosen due to their availability in the market. However, Raspberry Pi does not read analog input. Although it is coupled with ADS1115 (16-Bit 4-Channel Analog-to-Digital Converter (ADC)), the desired performance is not attained. Therefore, a sensor which has directly digital output configuration is sought and Polulu's Magnetic Encoder is elected. Yet, its connection is not suitable for existing DC-motors hence, low-power micro metal gear motors interchange motors. However, modifications on the electronics do not lead to a successful circuit. 4

motors can be run simultaneously but not in a controlled fashion. Further investigations lead the conclusion that Raspberry Pi Zero cannot run 4 motors in a controlled manner as an Arduino is. Pi has a user interface and working principle as the personal computers. Even though it can execute custom codes, it is not a real-time process. Any change in the structure of the control code or any interface, which may even not visible to the user, behind the pi's operating systems differentiates the execution time and response, which sabotages the control of motors. Then, motor-drive board is separated from the camera board.

The motor drive unit consists of Arduino Promicro, 4 DC motors (136:1 Sub-Micro Plastic Planetary Gearmotor), 4 Bourns Infinite Rotary Sensors, 2 L293DD h-bridge and 5v Step Up-down voltage regulator. Raspberry Pi and Pi Camera form the motherboard, and it is connected to Arduino by UART protocol. A 7.4 V Li-Po battery powers both boards through a voltage regulator. Pi is in charge of camera imaging and having navigation commands from the operator and pass to Arduino while Arduino controls the motors given by Pi commands.

2.4.2 PCB Fabrication

The components presented in the previous section are structured and assembled on Printed Circuit Boards (PCBs) which are designed individually. Initial versions are fabricated in a lab environment, whereas later designs are custom-manufactured.

PCBs are fabricated on flexible i.e., Dupont Pyralux, copper (Cu) coated Kapton sheets or hard i.e., FR-4 copper covered plates. Both materials are used for different designs yet the fabrication procedure for both is exactly the same and as follows. First of all, copper is covered with a photoresist material, i.e., mat nail polish. Then, the coated plate is placed under Universal Laser Systems VLS 3.50 laser engraver to ablate excessive nail-polish around pads and traces. Later, the plate is dipped into an etchant solution of H_2O_2 and HCl to remove accessible Cu to expose traces. Finally, remaining nail-polish and other molecules are cleaned by acetone and it is ready to be soldered. Custom-manufactured PCBs are also

fabricated by a similar procedure yet in a production line. In Figure 2.28, output of the process is represented.

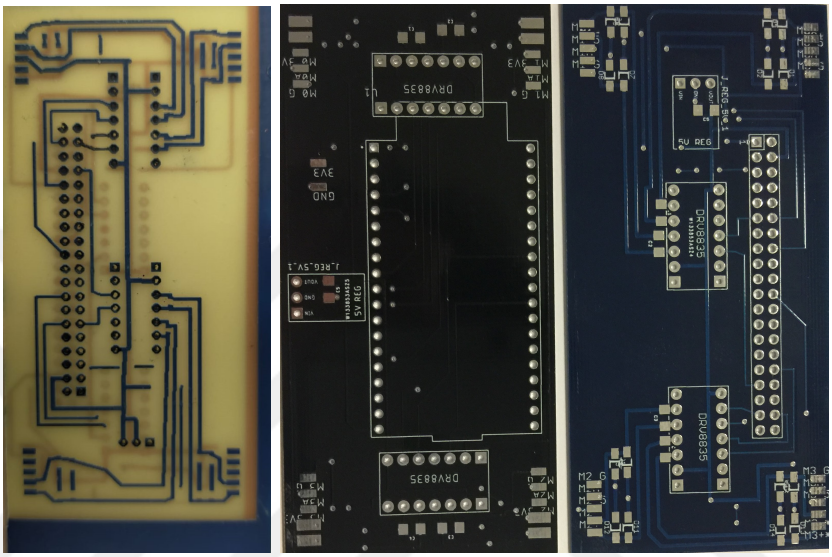

(a) (b)

Figure 2.28: (a) Fabricated PCB in lab by lithography (b) Fabricated PCB by custom-manufacturing by lithography.

Chapter 3

Design and Manufacturing of FAWSCY

In this chapter, the final version of FAWSCY is discussed. A novel wheel design is presented. Modification on the body and circuitry is explained. Finally, assembly guide is presented.

3.1 Wheel

Through all wheels and legs that run the robot, the bellow wheel was the most promising one. However, adjusting its wheel length in the existing configuration was over-challenging. Therefore, a novel wheel design that is working with a similar adjusting principle is presented.

The new wheel should be adjustable by its length while keeping its diameter constant. Hence, either wheel units should be sliding through each other, or the wheel itself should be deformable to contract and expand. Bellow wheel was an example of a deformable one and although it was a strong candidate, it failed. Therefore, a slidable design is wise to implement. For this, a modular novel design

is inspired by wickers. Figure 3.1 represents the modularity of wheel. There exist two bases for bottom and top, where the next unit can be connected to previous units by u-folds. There lies the prism between the bases to give strength to the module while shaping its fibrils to wicker. The prism points outwards and u-locks are folded inwards to create a smooth surface so that sliding of prisms on the top of bases is not impeded. Lastly, on the top, a trapezoid is formed from the top base and folded 90° inwards to connect the wheel to the hub and the lid. Figure 3.2 displays folded and wickered modules. The first and the last units are linked to get the circular shape. The main part of the wheel is wicker PET modules, yet it is not enough to implement into the robot. Cylinders are needed to be enclosed by hubs and lids, which are demonstrated in Figure **??**.

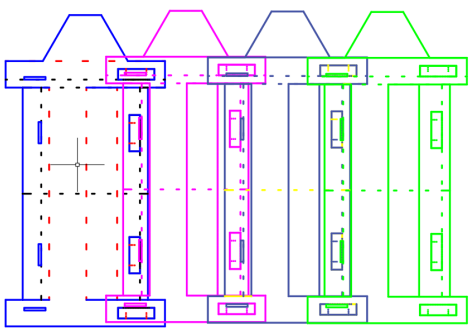

Figure 3.1: Sequence pattern of the wheel. On the 1^{st} one, blue solid lines are cut lines and red dashed lines are crease references. Pink, green and grey ones are to visualise sequence.

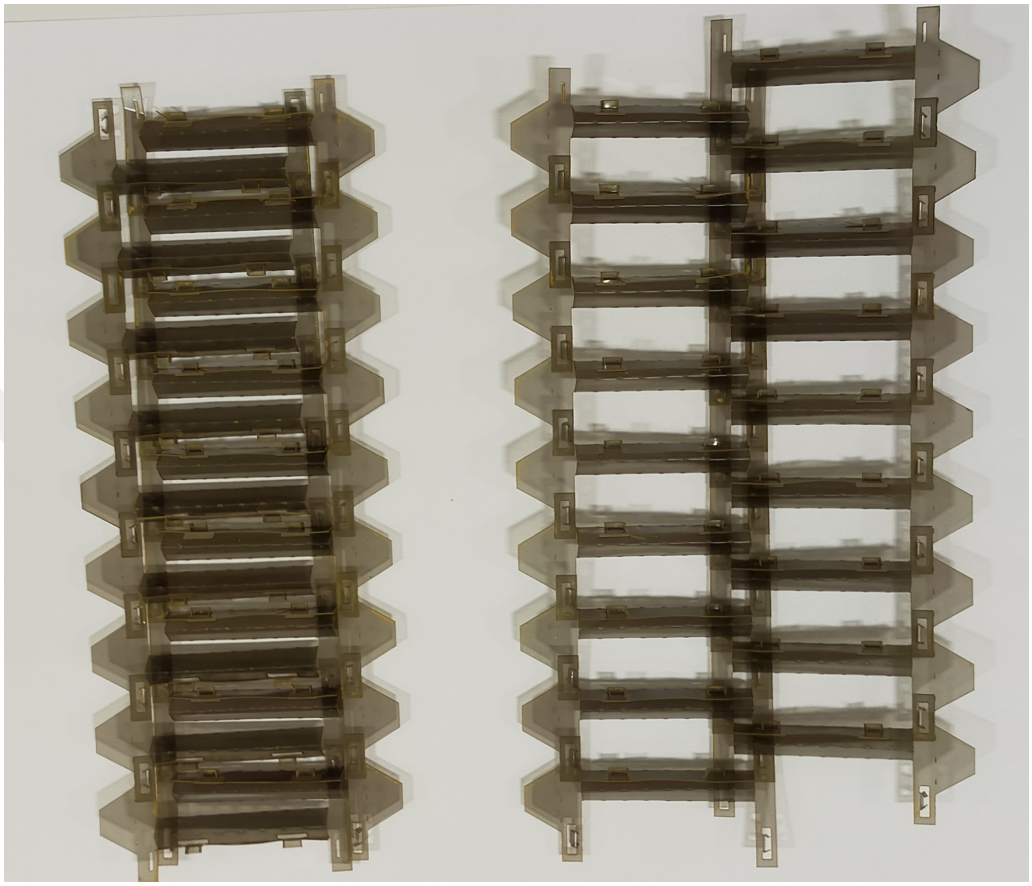

(a)

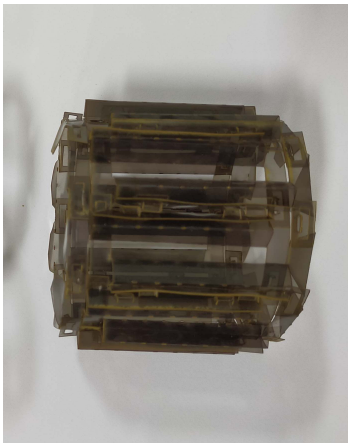

(b)

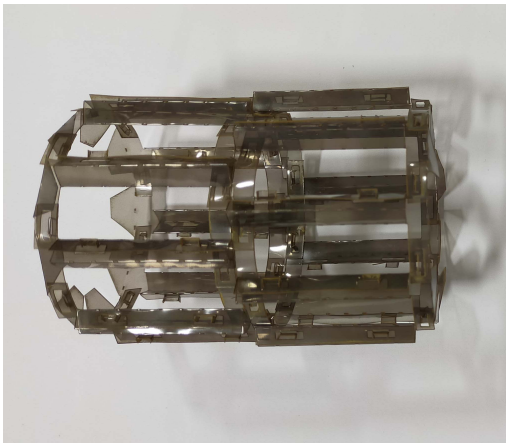

(c)

Figure 3.2: (a) 9 units of the module connected to each other and its symmetric cut to complete its wickered form. They are cut and folded from PET sheet. (b) Circled compact form. (c) Circled loose form.

The layers of the wicker wheel can slide through each other, resulting in different lengths. Therefore, a mechanism to accomplish this sliding motion is needed. It is usually done in deformable origami wheels by squeezing the wheel from two sides through the centre [32]. However, this solution is not applicable to FAWSCY. The better solution would be to pull it from one direction in a controlled manner and it also needs to be reversible. In literature, those mechanisms are called tendon-driven mechanisms yet; they are used for mainly wearable bio-robotics, i.e., gloves [46–48]. A similar mechanism is used by [49] for a running-jumping miniature robot, by pulling a strip connected to the foot to store potential energy so that it can jump by release. Hence, to create a tendon-driven mechanism, a string is connected to the lid, and it flows through the hub and ends on the spool represented in 3.3.(d) as a single thread. The spool is directly connected to the actuator. As an outer cylinder to string, a spring is also connected from lid to hub to open the wheel back, and guiders for spring are added as the second outer shell to ensure that spring deforms on the only desired axis. They are displayed in Figure 3.4. Therefore, hubs and lids have inner cylindrical spaces for the flow of the string. They also have mortise to place and hold string guiders and grove to place the string. Hub, additionally, has bearing bedding and extension shaft to connect to the body. Figure 3.5 demonstrates the wheel in assembled form with its inner mechanism, hub and lid, and folded wicker outer PET sheets, and it weighs about 23 gr. Lastly, strings' addition is navigated the drive mechanism from wheels directly connecting to dc motors to geared drive mechanism. Hence, hub and camshafts are added gears that couples to each other. Figure 3.3.(c) also shows the camshaft.

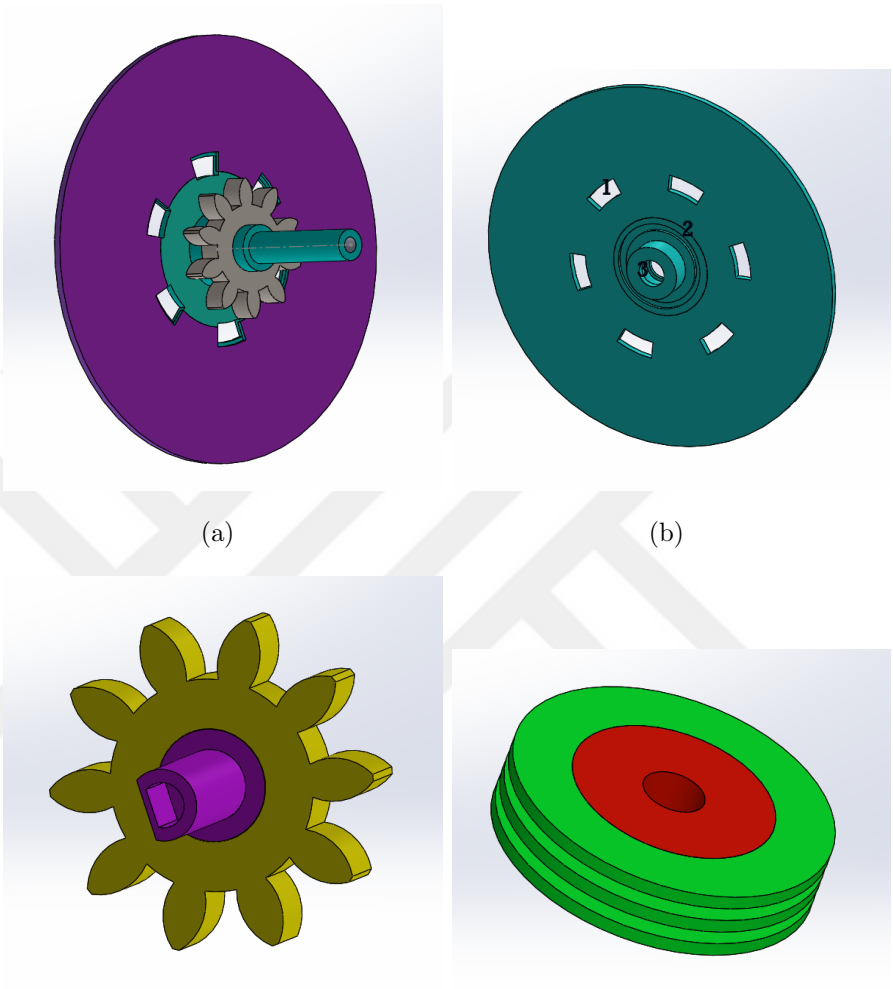

(a) (b)

(c) (d)

Figure 3.3: (a) Hub with gear. Purple : flexible material(TPU) and green : hard material (PLA), beige: polyamide gear (b) Lid: flexible material (TPU). 1: mortise to connect guider, 2: lid bedding, 3: bearing nest. (c) Cam Shaft of the wheel, shaft is PLA printed, gear is polyamide milled. (d) Spool connected directly to stepper motor to wrap strings, red: TPU, green: PLA

(a) (b)

Figure 3.4: (a) Wheel inner mechanism SOLIDWORKS files : 1: Lid, 2: Spring Guider for Lid, 3: Spring Guider for Hub, 4: Hub, 5: Gear (b) Printed lid, Lid Spring Guider, Hub Spring Guider and assembled spring

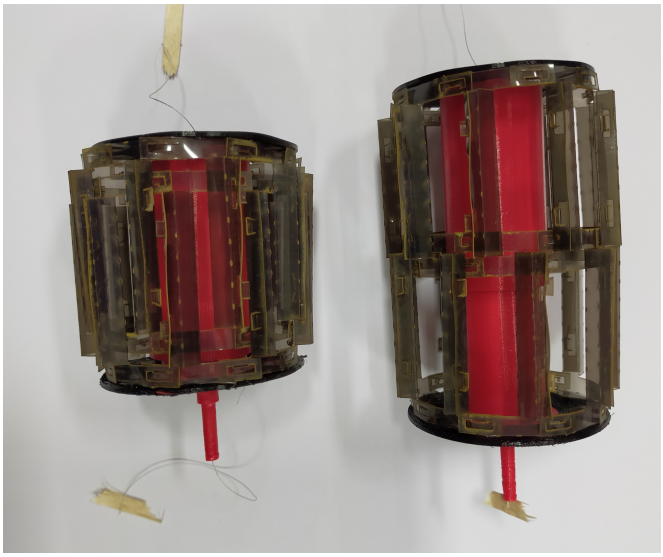

Figure 3.5: Assembled form of Wheel (a) closed form, short in length, (b) open form, long in length

Another desired feature of the wheel is to be able get constant processable camera outputs, i.e. videos or instant images. Hence, during various experiments, images from its pi camera are taken and presented in Figure 3.6. Although there exist blurred images, yet transition lines are distinct and objects are distinguishable. Thus, the wheel is acceptable.

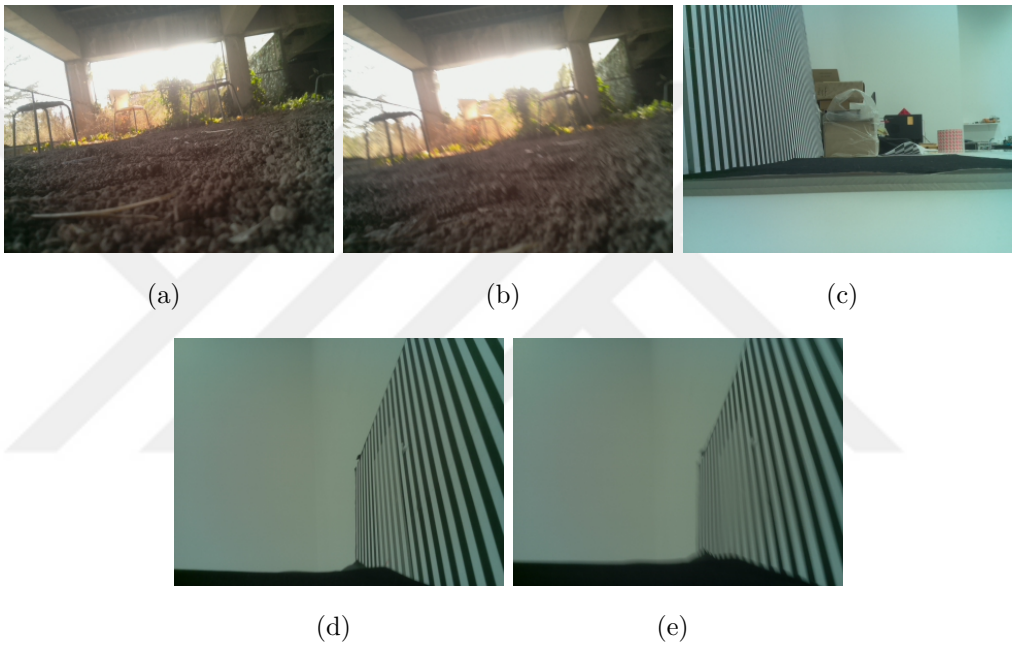

Figure 3.6: Image samples taken by the robot during experiments. (a) clean gravel terrain (b) blurred gravel terrain (c) obstacle scaling (d) clean inclined surface climbing (e) blurred inclined surface climbing

3.2 Body

Designing an origami-inspired body benefits the robot by reducing its weight, adding resilience to collisions and drops, increasing the robot's durability. Moreover, it is low cost and easy and fast to manufacture. However, it also has disadvantages, such as the parts' alignment is not guaranteed as it can deform without failure. In the previous chapter, discussing different leg, wheel and body

solutions, this issue is mentioned. For the final body, it is desired both to benefit its advantages and avoid its possible problems. Hence, the foldable body is designed aiming; it should keep the integrity of parts and act as a closure from damages and disturbances. Thus, the same design principles are applicable, yet it is in a more straightforward form. As Figure 3.7 exhibits, it is again 3-layered to provide enough room for parts, yet it has one T-fold on each layer to form the frame and is mostly cut to provide the transition between layers.

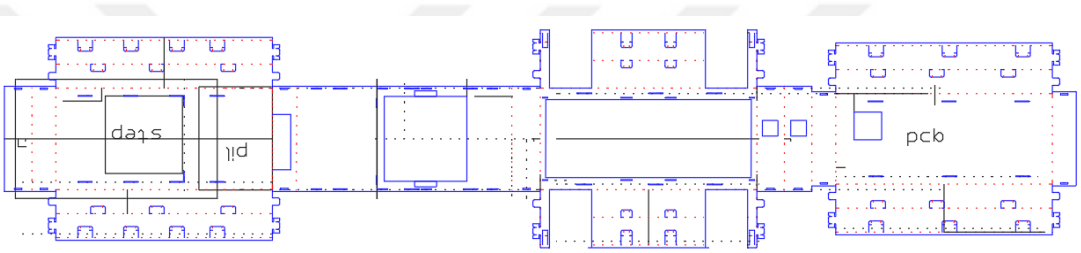

Figure 3.7: FAWSCY's final AutoCad design.Folded form weights 11.3 gr.

Another significant element of the body is length adjustment mechanism of the wheels. As it is explained in Section 3.1, it is consisted of a string mechanism flows through from lid of the wheel to the spool. Hence, its alignment should be kept. Moreover, it is already known that the alignment of dc motors and rotary sensors also should be also maintained. Hence, existing motor casing is extended to cover dc motors and actuation mechanism of wheel length adjustment. Also, as driven mechanism is altered from direct to gear-set, motor casing have bearing holes to mount hub extension. Figure 3.8 represents extended casing, used roller bearings and spool, again to resemble completeness.

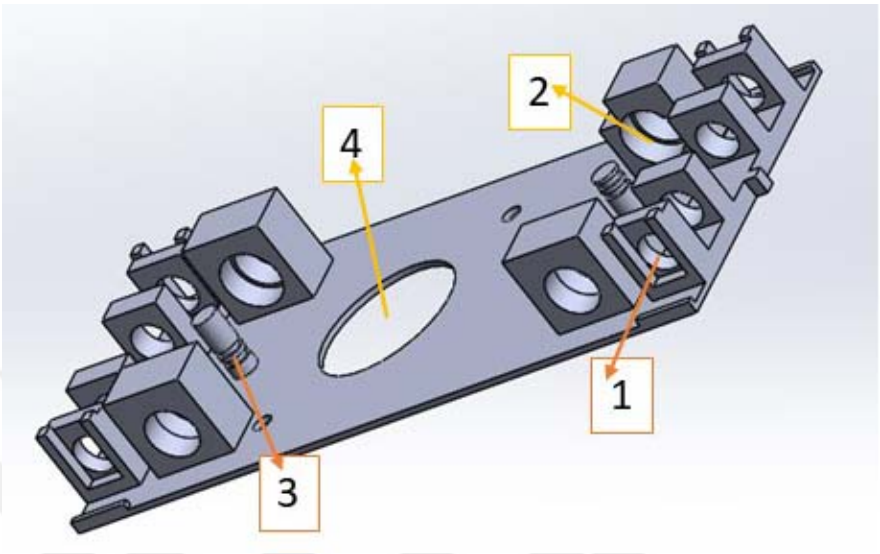

(a)

(b)

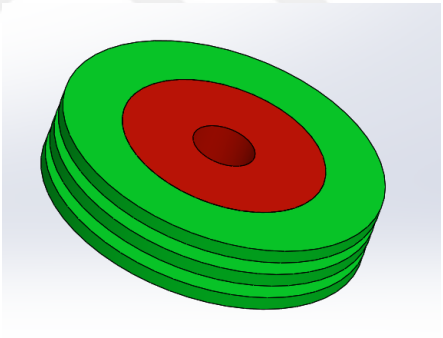

(c)

Figure 3.8: (a) Motor casing, 1: dc motors and rotary sensors, 2: bearing bedding, 3: string guider to spool, 4: spool actuation motor bedding and spool connection point (b) Roller bearing to connect wheel hub to casing (c) Spool connected directly to stepper motor to wrap strings, red: TPU, green: PLA

3.3 Electronics and Control Algorithm

3.3.1 Electronics

For the final version of FAWSCY, the two-unit integrated circuit is remained as a motor drive unit and camera unit, yet modifications are implemented by present needs. It is still run by 4 individually controlled motors. Additionally, it has one stepper motor to adjust the length of wheels simultaneously. In other words, in an instant, there exists only one length configuration for all 4-wheels. As it also requires accurate timing, the stepper motor is also coupled with Arduino motor drive unit. To provide output pins on Arduino for stepper, DC-motor driver bridges are also switched. The stepper motor and remaining system are powered separately due to the stepper motor's current drawn rate. The Stepper motor is powered by a 7.4 V Li-Po battery. Meanwhile, the system may be powered 3.7 V Li-Po battery and FAWSCY runs about 20 mins, max, or 7.4 V and the robot runs about 1 hr.Moreover, a current and voltage sensor, INA219 is coupled with Raspberry Pi through I2C protocol to record the power consumption of the robot on running. The sensor has %1 precision band and by 12-bit ADC, it can read up to $\mp$3.2A with 0.8mA resolution [50]. Table 3.1 lists the electronic components and Figure 3.9 represents the final PCB layout.

Table 3.1: Electrical Component List of FAWSCY

COMPONENT	QTY
Raspberry Pi Zero W	1
Pi Zero Camera	1
Arduino Promicro	1
700:1 Sub-Micro Plastic Planetary Gearmotor	4
Bourns Infinite Rotary Sensors	4
DRV8835 Dual Motor Driver	2
Sanyo Pancake Bipolar Stepper Motor	1
DRV8834 Low Voltaje Stepper Motor Driver	1
INA419 Current Power Sensor	1
5V Step Up/down Voltage Regulator	1
LF33ABV 3.3 V Regulator	1
7.4 V Li-Po Battery	2

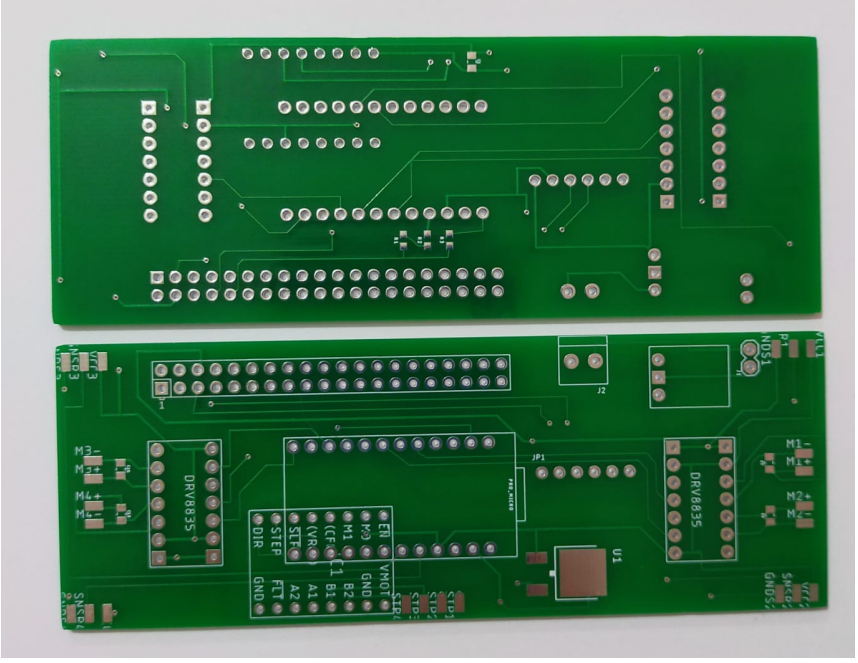

Figure 3.9: Final fabricated PCB of FAWSCY

3.3.2 Control Algorithm

After the separation of motor driver and camera circuits, the control algorithm is also divided into 2 parts. The base C++ Arduino code for motor control is inherited by Askari's work [11] and improved by navigation commands for DC motors, i.e., forward, reverse, turning forward left, turning reverse right, clockwise turn around itself, etc., stepper commands and communication with Raspberry Pi via UART protocol. On the other hand, Raspberry Pi takes input from user for navigation command, including stepper command; then passes the command to Arduino, records videos and logs navigation commands, and tracks power consumption through INA219.

3.4 Assembly

Fabrication of wheel and body parts are discussed previous sections in detail, hence Figure 3.10 demonstrates how the parts are assembled to form FAWSCY. The PCB (which is not shown in figure) shown in Figure 3.9, is placed on the top of motors and string spools in Figure 3.10.(a) whereas the batteries resides next to stepper motor Figure 3.10.(b).

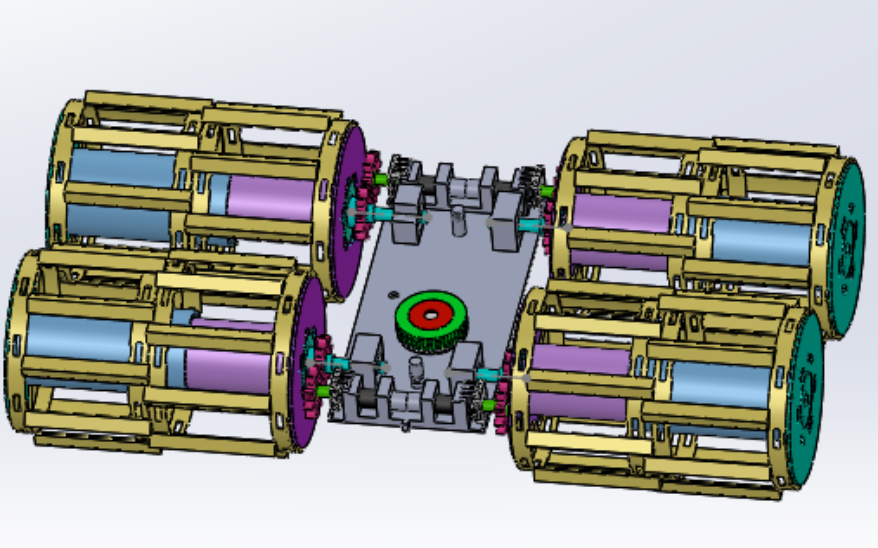

(a)

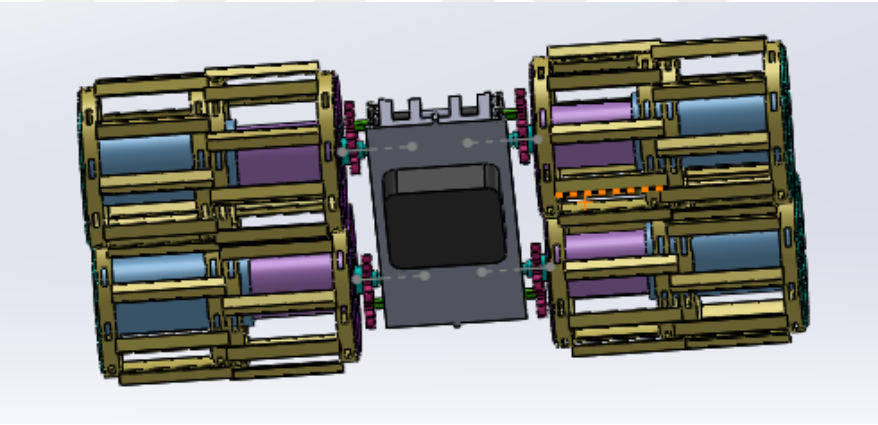

(b)

Figure 3.10: Assembled robot with its dc and stepper motors, rotary sensors, gears, camshafts and wheels

Chapter 4

Tests and Evaluations of FAWSCY

As it is discussed in Section 3.4, FAWSCY is assembled and its running and resilience tests are conducted. Experiments are divided into 5 different categories as obstacle climbing, inclined surface climbing, different terrain runs and fall tests to examine that it can perform under different conditions and disturbances, and different wheel length combinations to assess possible effects on running.

4.1 Various Terrain Running

FAWSCY is mainly designed to continue performing on various terrains and with unexpected disturbance. Thus, tests are started with its running performance. To represent the indoors and outdoors of city centers, i.e. pavements, roads, etc., lab environment is used, then running on gravel, soil and grass are conducted as rough terrain experiments.

4.1.1 Smooth Ground

The very first analysis done on FAWSCY is its running performance in indoor environment or smooth ground such as lab floor, corridors, or marble surfaces. Initially, it is verified that it can respond to navigation commands, i.e., it can run forward and reverse directions, and it can turn to any direction, including around itself. Moreover, those tests are conducted under Motion Capture system so that visual inspection and tracking data are available. Hence, Figure 4.1 and 4.2 show frames of forward, turning right and left runs, and clockwise (CW) or counter-clockwise (CCW) turns respectively by Motion Capture system which is recorded in MJEP mode. The desired tasks are achieved as visual inspection, and tracking data also affirms that tasks are completed. Figure 4.3 explains forward run whereas 4.4 demonstrates turns in any direction achieved as expected. Run experiments also investigate short and long wheel configurations. As Figure 4.5 displays the power consumption, closed and open wheels have equal contribution to the robot's running performance. Additionally, Figure 4.6 displays how FAWSCY closes its wheels.

Additionally, it is needed to investigate whether FAWSCY maintains its run after a collision. As it is presented in Section 1.3, it should be able to collide with living and non-living subjects without any harm. Hence, it is crashed with people. Although its trajectory has changed, it preserves its motion and is presented in Figure 4.7. Thus, it successfully satisfies the main requirements.

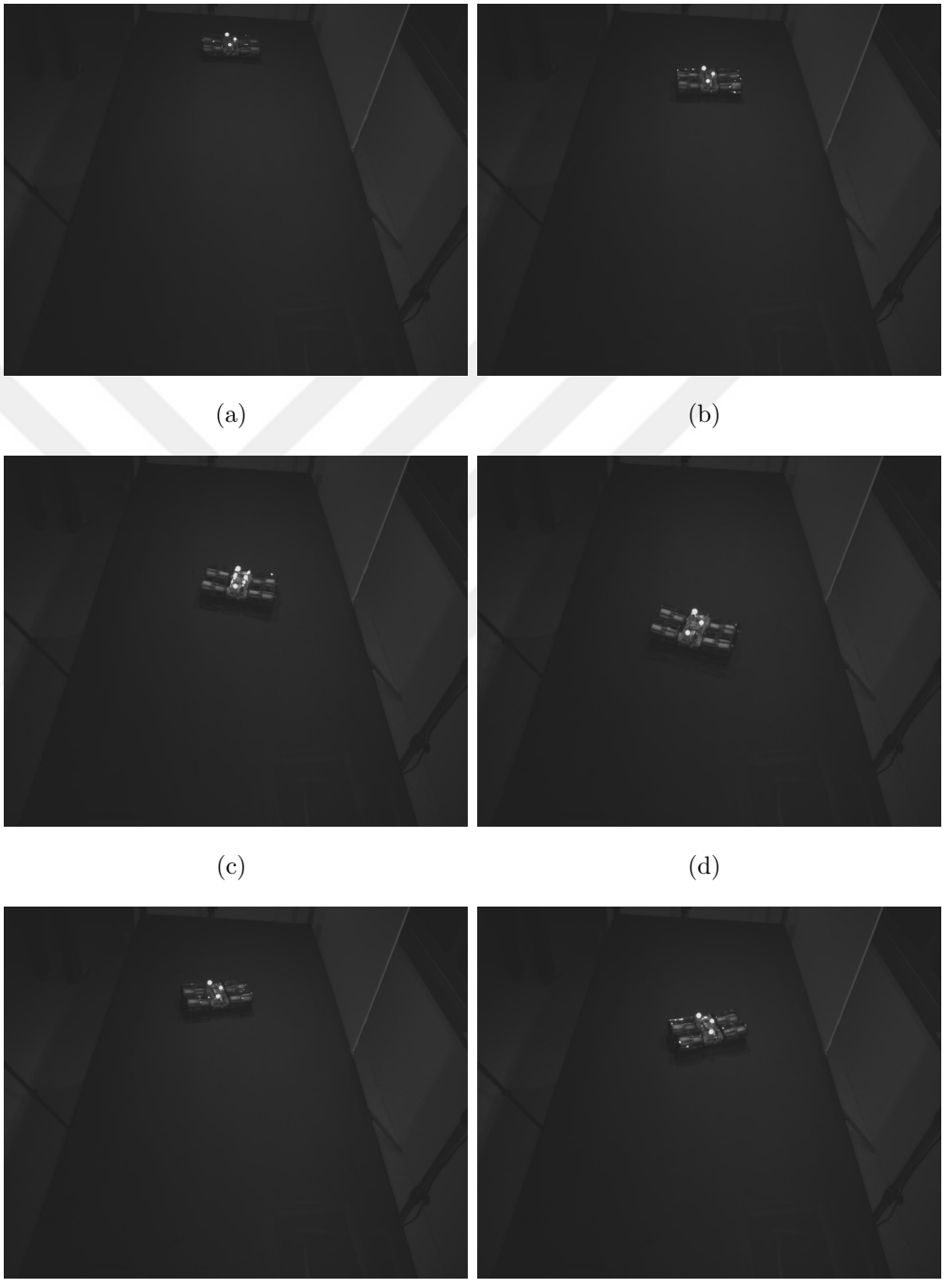

(a) (b)

(c) (d)

(e) (f)

Figure 4.1: First row represents respond of forward navigation command under Motion Capture System. Second and third rows represents right and left turns respectively. It does not have instant turns as the motors run at low frequencies, $0.6Hz$.

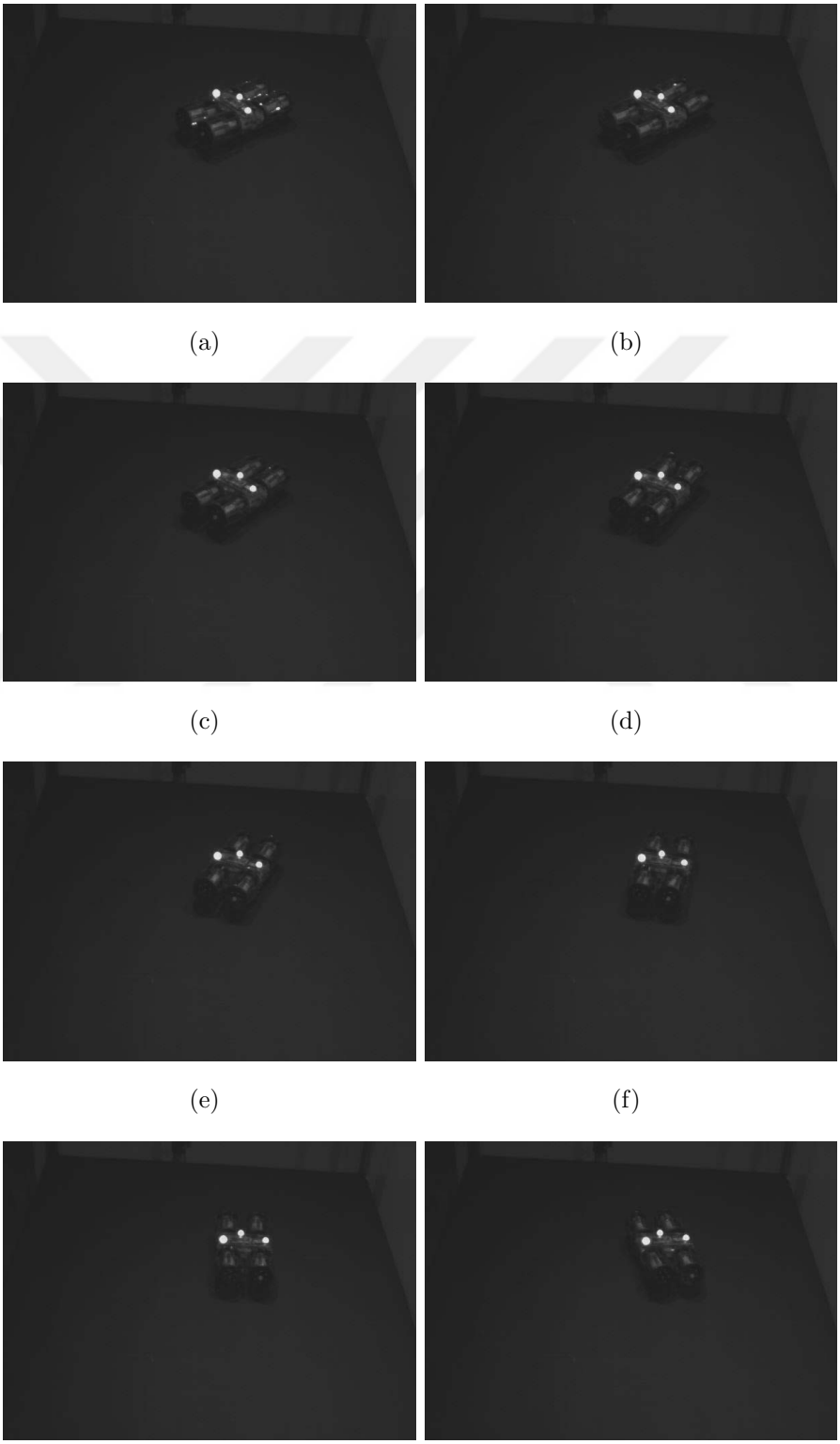

(a) (b)

(c) (d)

(e) (f)

(g) (h)

Figure 4.2: Clockwise (CW) turn around itself under motion capture system.

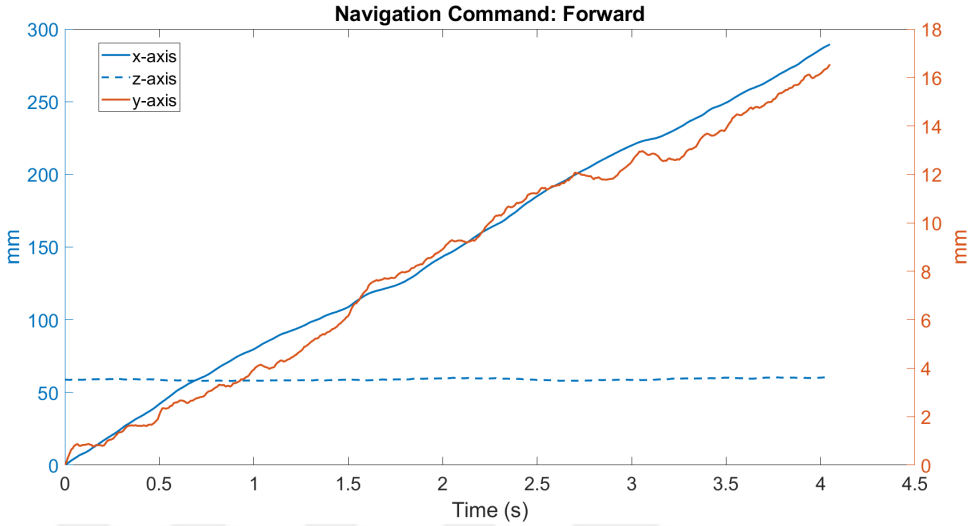

Figure 4.3: It does not maintain a perfect line along y-axis, which means it has deviations as it does not have a restricted position control on wheels but only velocity control of motors. Yet, transmission through gear sets on wheel-motor couples is not guaranteed as identical. In miniature scale, any tiny effect can propagate. Nevertheless, oscillations around 15 mm is not that significant compared to robot's width as 185 mm for short wheels and 255 mm for long wheels.

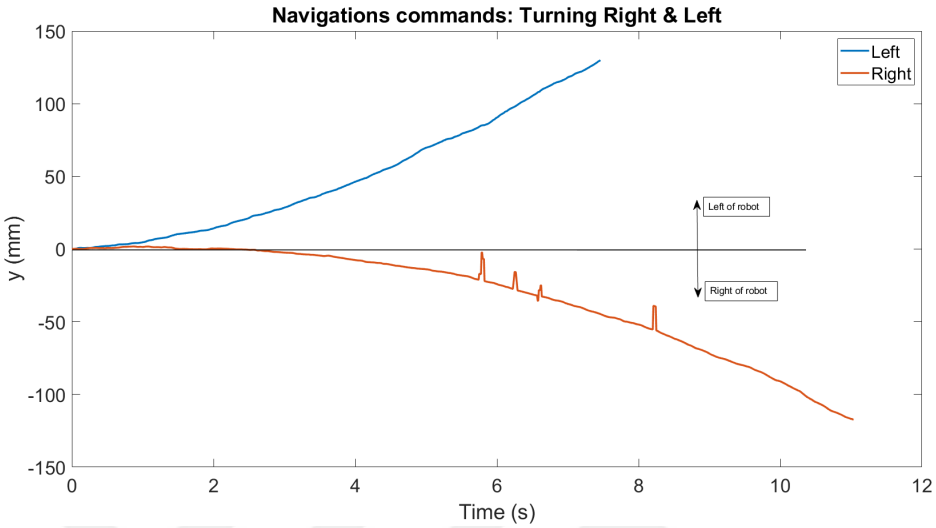

(a)

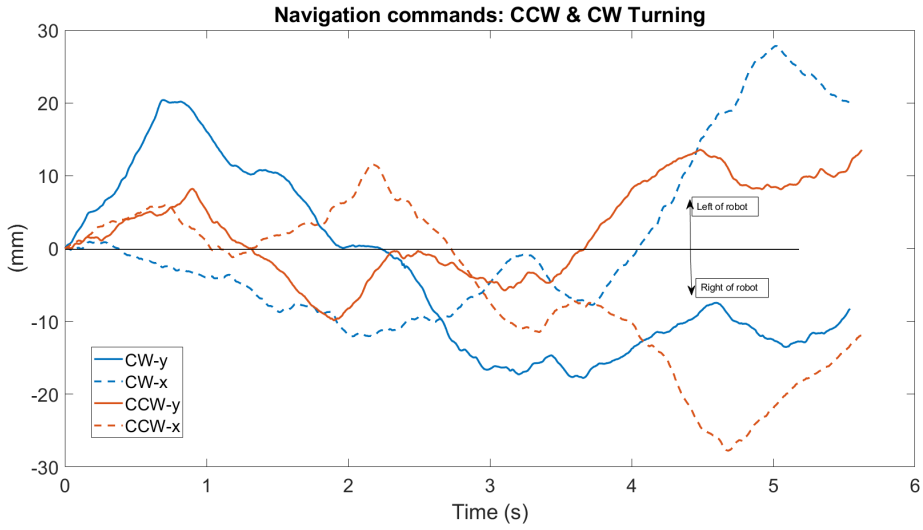

(b)

Figure 4.4: (a) Change of positions along y-axis under left and right turning commands. By the given commands, it changes its direction on desired sideç (b) Change of positions along x and y-axes of CW and CCW turns. Both in x and y axes it oscillates on sinusoidal fashion, as on the exact same point, it changes only its direction as expected.

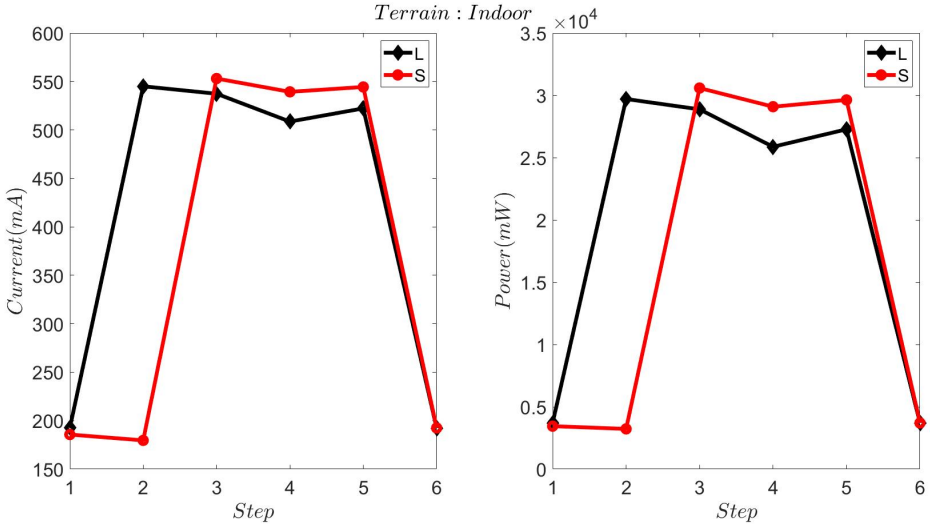

Figure 4.5: Current and power consumption of robot during Indoor Terrain Running.Legend express as L: long vs S: short wheel

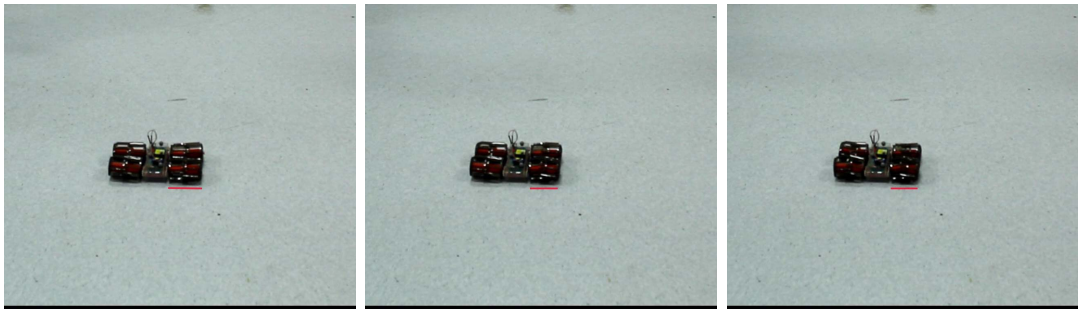

(a) (b) (c)

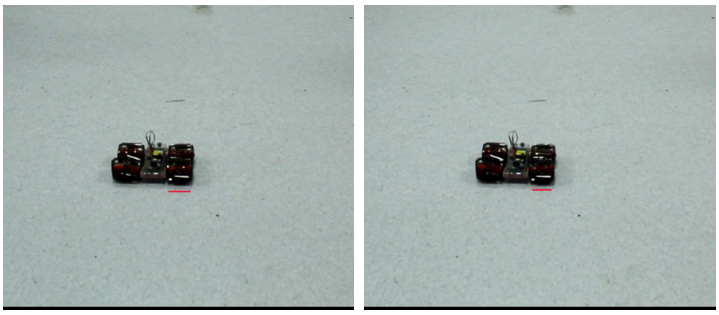

(d) (e)

Figure 4.6: Frames of wheels' length adjustment

(a)

(b)

(c)

(d)

(e)

(f)

(g)

(h)

Figure 4.7: Frames of how FAWSCY responds and preserves its motion under disturbances.

4.1.2 Gravel

For a miniature robot, one of the roughest and most dangerous terrains is gravel and rocky paths. Wheel-like locomotion parts are usually higher performance as it is discussed in Section 1.2 and 2.2.1. Hence, FAWSCY overcomes that challenge with its wheel design. In principle, gravel paths are similar to obstacles exhibited in Section 4.2, yet it is randomised version. It is randomised in height, width and sharpness, whereas obstacles in Section 4.2 are mere solid bars. This randomisation, for sure, affects the reaction of the robot through running yet, it only disturbs the linear path of the robot by randomised traction forces due to contact.

Figure 4.8 demonstrates the gravel terrain experiment environment and frames a few stages of the run. As expected, short wheels outperform long wheels as mainly they can keep continuous contact with the ground, and its spiky design can go over sharp edges and corners of gravels, while on long wheels, gravels can be stacked on the grids and spaces on the wheel. Hence, it is preferable to run on short wheels for this terrain as the robot can sustain running.

(a) (b)

(c) (d)

(e) (f)

(g) (h)

Figure 4.8: Test video frames to represent Gravel Terrain set-up and results, with closed wheels.

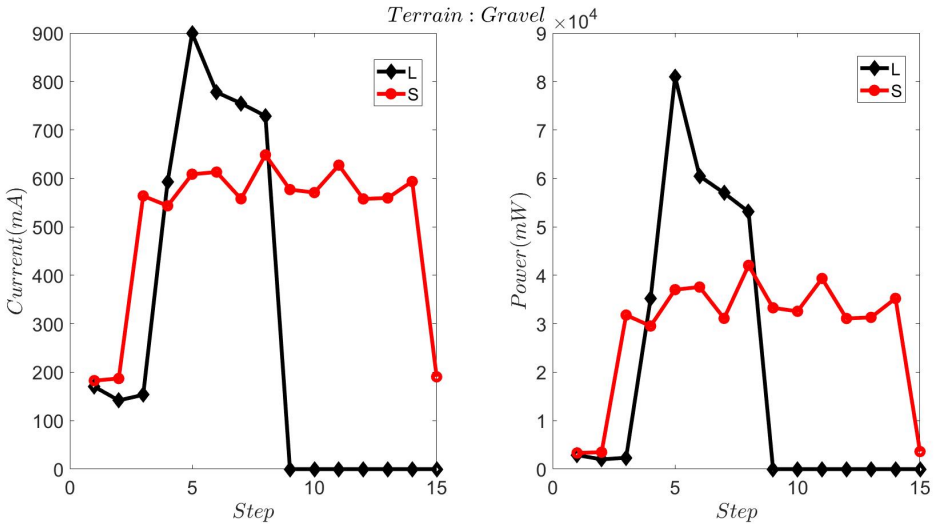

Figure 4.9: Current and power consumption of robot during Gravel Terrain Running.Legend express as L: long vs S: short wheel

4.1.3 Soil

The final rough terrain experiment is running on the soil. Although it is an outdoor terrain, soil exhibits similar characteristics to indoor environments for wheeled robots. It is smooth, it is soft and it can generate enough friction to run. Moreover, FAWSCY's wheels' generated pressure to sink on the soil is relatively low as its contact length to weight ratio is high compared to other miniature robots. For instance, both MiniAQ [11] and SMoLBot [12] have $0.5(20mm/40gr)$ contact length to weight ratio whereas FAWSCY has $1.15(320mm/278gr)$. Hence, it is expected that FAWSCY's both wheel configuration performs as desired on soil ground and experiments run are verified it. Figure 4.10 shows the soil terrain experiment environment and frames a few stages of the run. Also, Figure 4.11 displays the power consumption of the runs to prior one wheel length to another for having a longer duration of operation, and it appears that the long wheel is more efficient. When the wheel is on short configurations except for the spikes, the wheel has two cylindrical constant contacts with the soil from the sides of the hub and lid. On the long wheel, the middle line creates extra third cylindrical

constant contact, which increases the contact area, decreasing the pressure on the wheel, allowing a more pleasured ride.

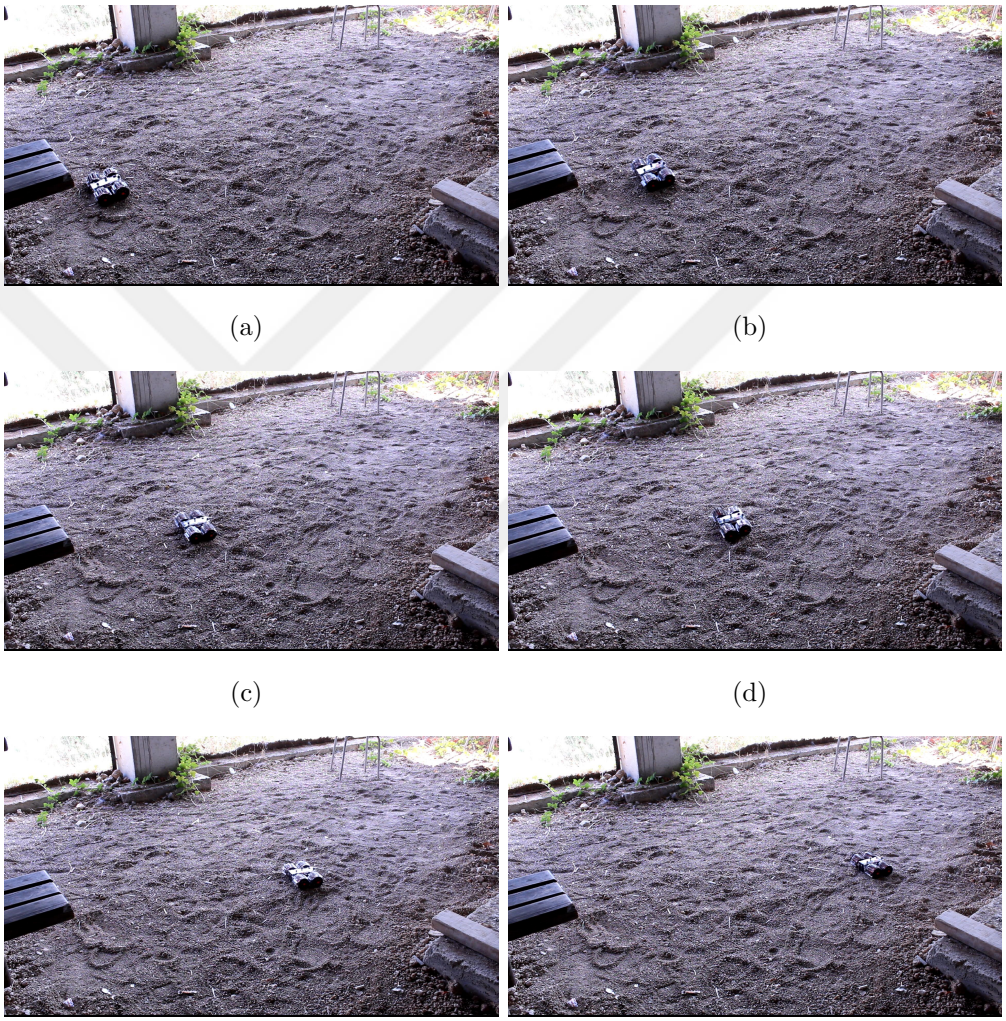

(a) (b)

(c) (d)

(e) (f)

Figure 4.10: Test video frames to represent Soil Terrain set-up and results, with closed wheels.

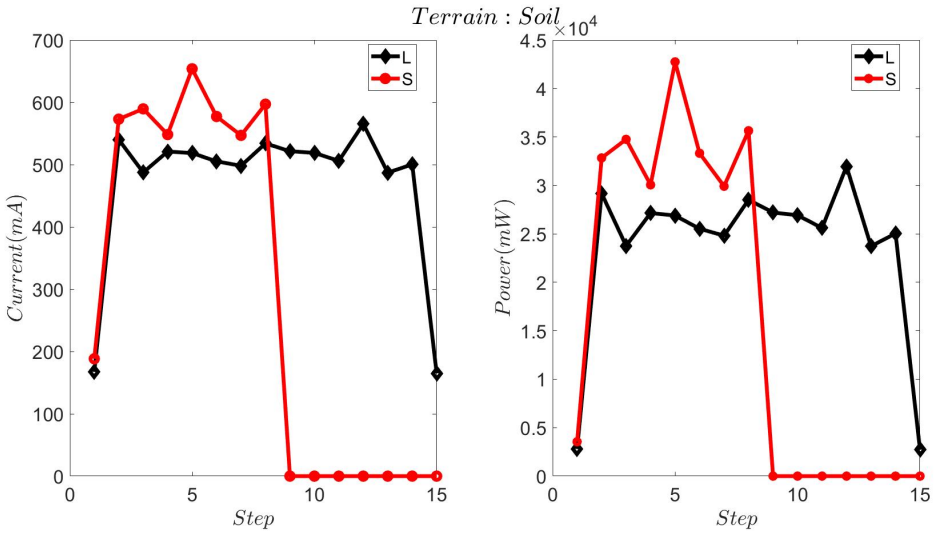

Figure 4.11: Current and power consumption of robot during Soil Terrain Running.Legend express as L: long vs S: short wheel

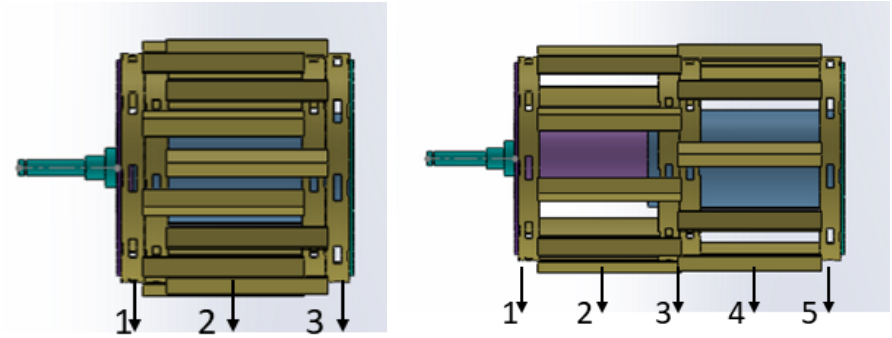

(a) (b)

Figure 4.12: Contact points (a) on short wheel, (b) on long wheel

4.1.4 Grass

Another rough outdoor terrain a miniature robot can come across is grass. For giant robots, it may not affect the robot's performance yet; in miniature robotics, generated forces affect more the robot, and terrain particles would penetrate into a robot and affect its performance in the case of grass. The grass is a fibrous terrain,

and these fibrils are fixed on one side while free to the other, which means until the robot evades those fibrils, it generates high instantaneous forces. In FAWSCY's grass terrain experiments, similar effects are observed. As discussed in Chapter 3, its drive mechanism consists of gear pairs and gears are not covered by PET body. Those grass fibrils enter into the gear set and impede its rotation temporarily or permanently. Another penetration point of fibrils is modules of wicker wheels. The module itself is formed by folding; therefore, there exist spaces that fibrils get into. Also, modules are connected to each other, and in closed form, the most compact configuration is attained, creating many tiny wedges for fibrils to get caught in. On the other hand, the open form has more spaces to fibril slide through without caught, hence it outperforms the closed wheel on grass terrain. While Figure 4.13 demonstrates the grass terrain experiment environment and frames a few stages of the run, Figure 4.14 supports the claim by exhibiting the power consumption. Short wheel consumes more power for a longer duration as it is struggled to continue.

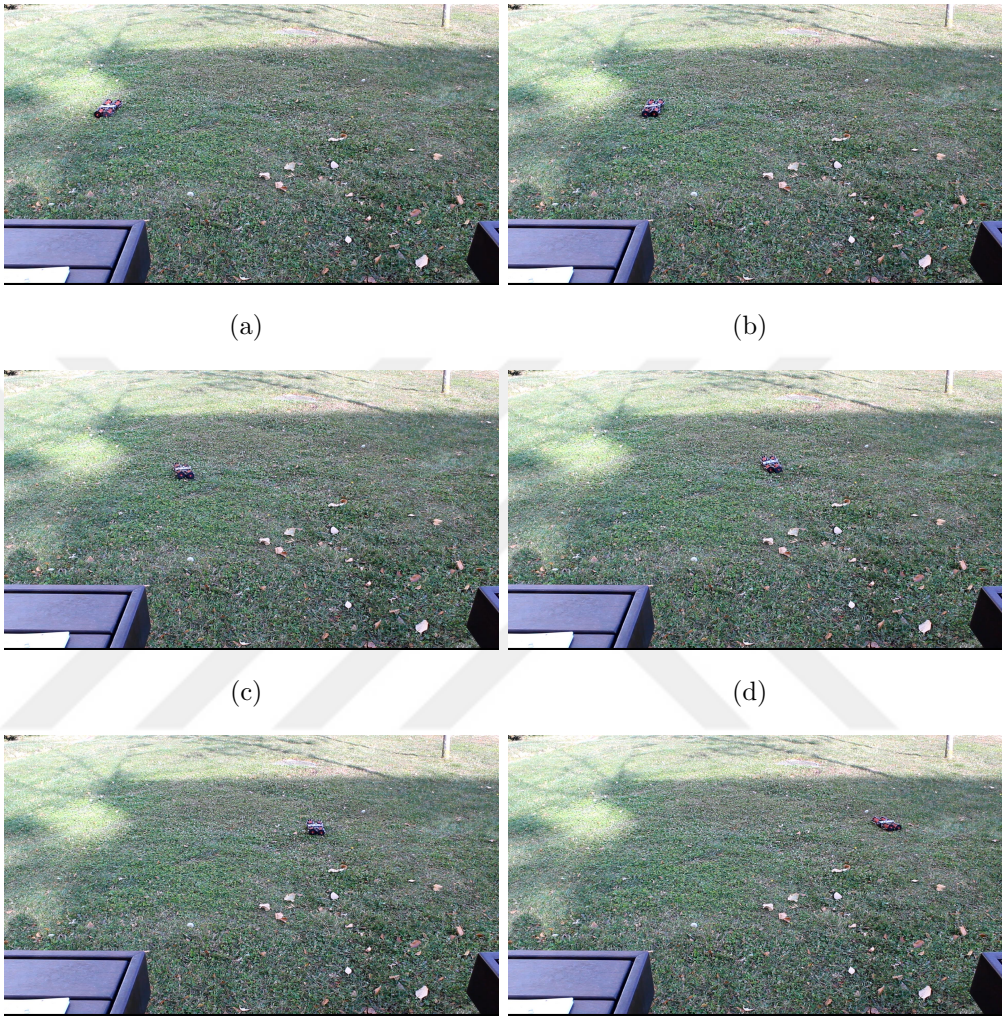

(a) (b)

(c) (d)

(e) (f)

Figure 4.13: Test video frames to represent Grass Terrain set-up and results, with open wheels.

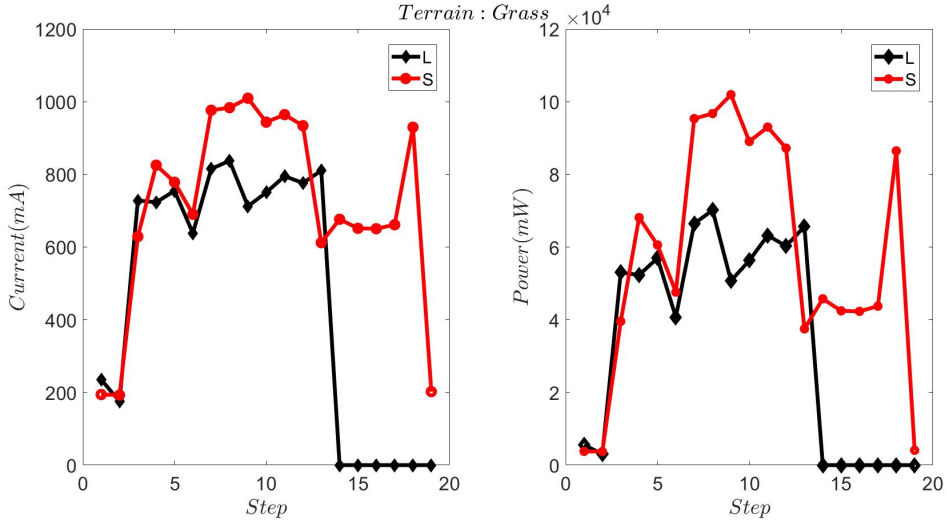

Figure 4.14: Current and power consumption of robot during Grass Terrain Running.Legend express as L: long vs S: short wheel

4.2 Obstacle Scaling

After runs, interactions with obstacles of FAWSCY are studied, whether it can pass or on which conditions it can get across the obstacles, and in which wheel length it exhibits higher performance. Therefore, one concrete barrier and one stair-like barrier with different heights are built. Figure 4.15 presents the concrede obstacles as a single layer on a definite height and how the robot runs over it by the frames of the experiment video, whereas Figure 4.16 exhibits the stair-like obstacles that rather than being one solid object, obstacle is a combination of various heights and widths. It also shows how its parameters are defined in the left-upper corner.

The robot is run through solid objects of height from 0.5 cm to 2.5 cm during the experiments. For stair-like case (in Figure 4.16 on top left corner, there exists a scheme to visualise stair parameters), obstacle's instant width (t) parameter is varied from 0.5 cm to 1.5 cm and its total height (h) parameter is varied from 1 cm to 3 cm. Experiments are resulted as the way that the short wheel in length

has better obstacle scaling capabilities. As Table 4.1 sums up, the long wheel can pass through only 0.5 cm, while the short wheel can pass up to 1.5 cm for solid obstacles. In case of stair-like non-uniform obstacles, it can climb narrower and longer configurations. As Section 3.1 explains the wheel design, the wheel has continuous sharp edges following each other which creates mechanical interlocking between the wheel and the obstacle. Yet, this interlocking is formed in a narrower area with continuous contact in the short form, therefore, has a higher traction force. On the other hand, in the long wheel, interlock strength decreases as a medium of contact is widened and appears discontinuous fashion. Also, Figure 4.17 shows its drawn current and power consumption for scaling cases that long wheel mostly consumes higher power or for longer duration as it tries harder to complete the task before failure. Additionally, Figure 4.18 is to better visualise interlocking for both length configuration.

Table 4.1: Highest achieved values on Obstacle Climbing for both Wheel Configurations

Wheel	Obstacle Height	Stair-Like Parameters
Short	1.5 cm	h: 2 cm, t: 0.5 cm
Long	0.5 cm	h: 2 cm, t: 1 cm

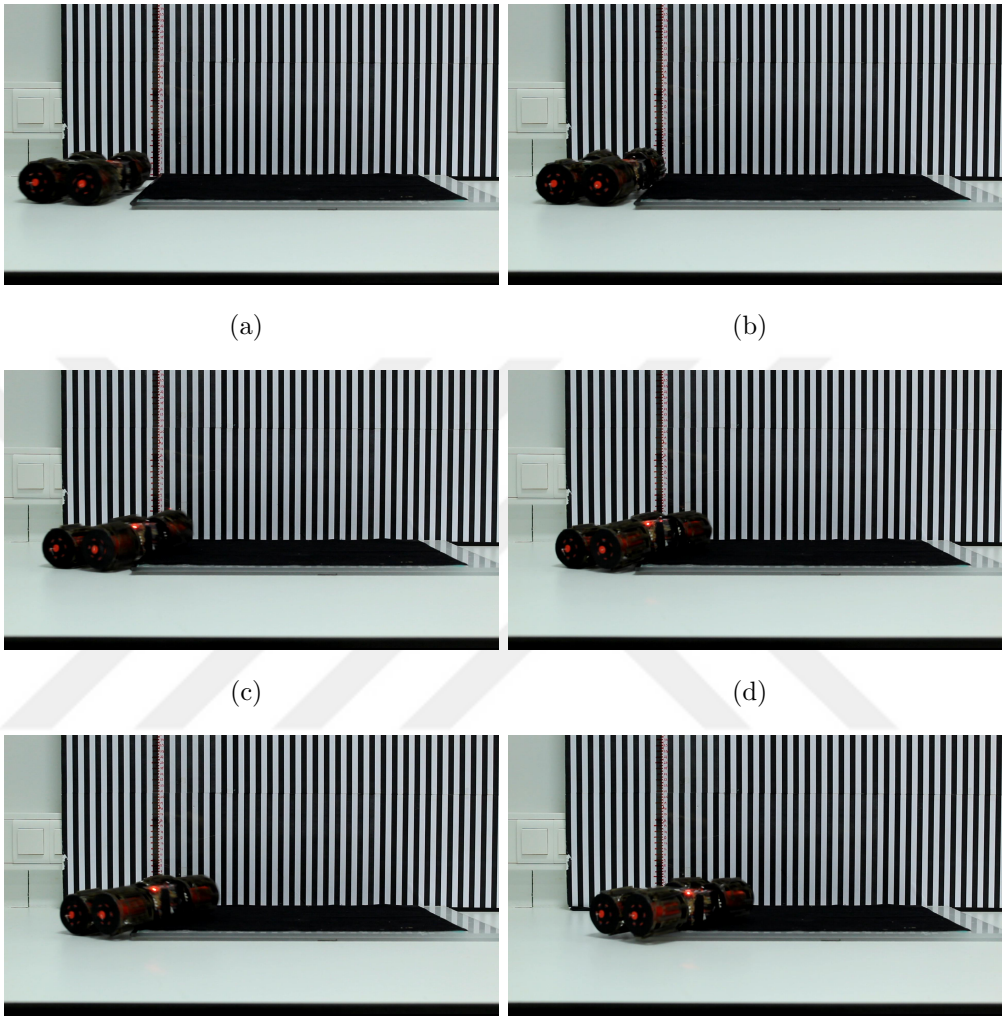

(a) (b)

(c) (d)

(e) (f)

Figure 4.15: Test video frames to represent Obstacle Climbing set-up and results, when height is $1cm$ with closed wheels.

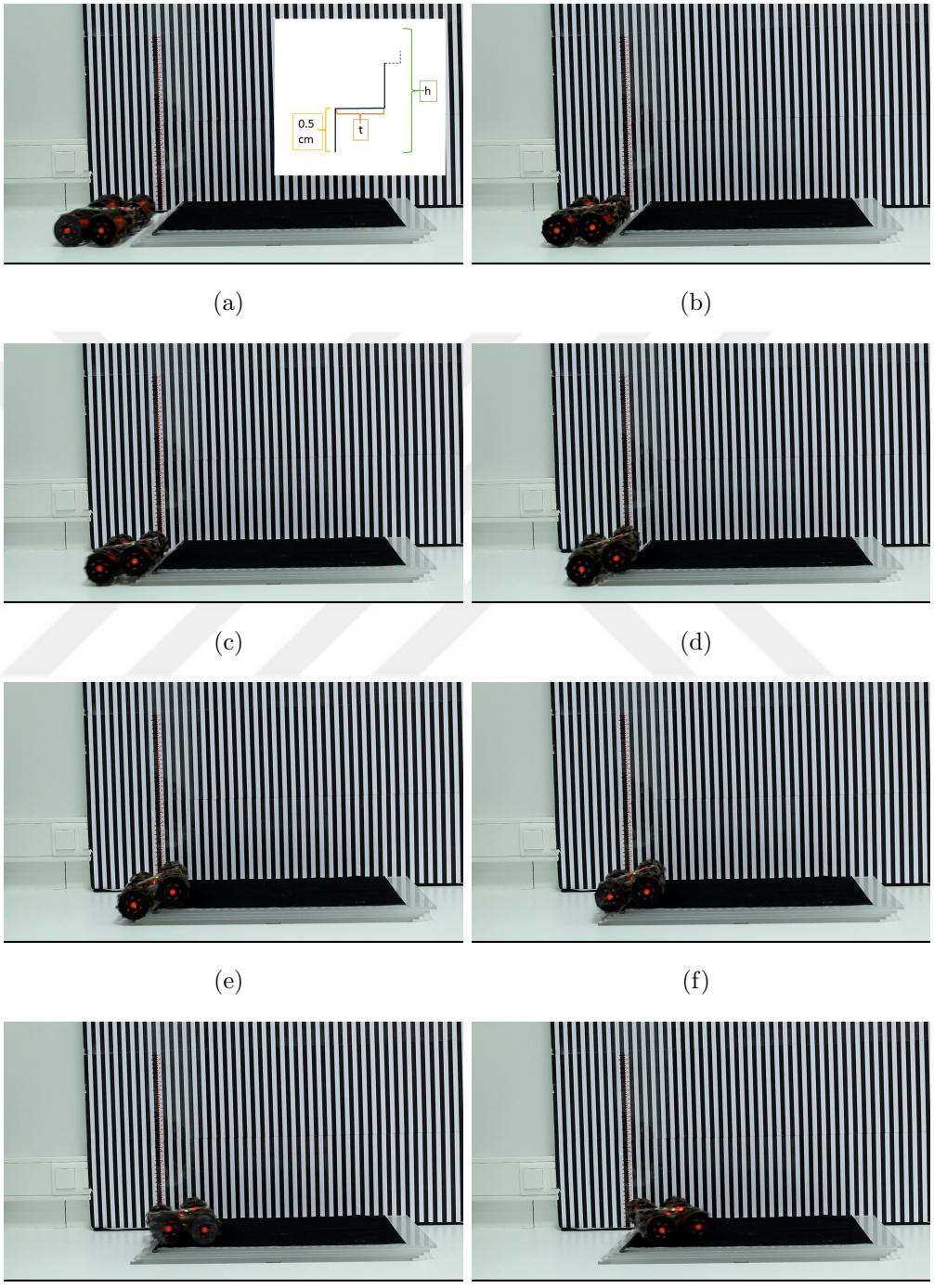

(a) (b)

(c) (d)

(e) (f)

(g) (h)

Figure 4.16: Test video frames to represent Stair-like Obstacle Climbing set-up and results, when stair width, $t = 1cm$ and obstacle height, $h = 1cm$ with open wheels.

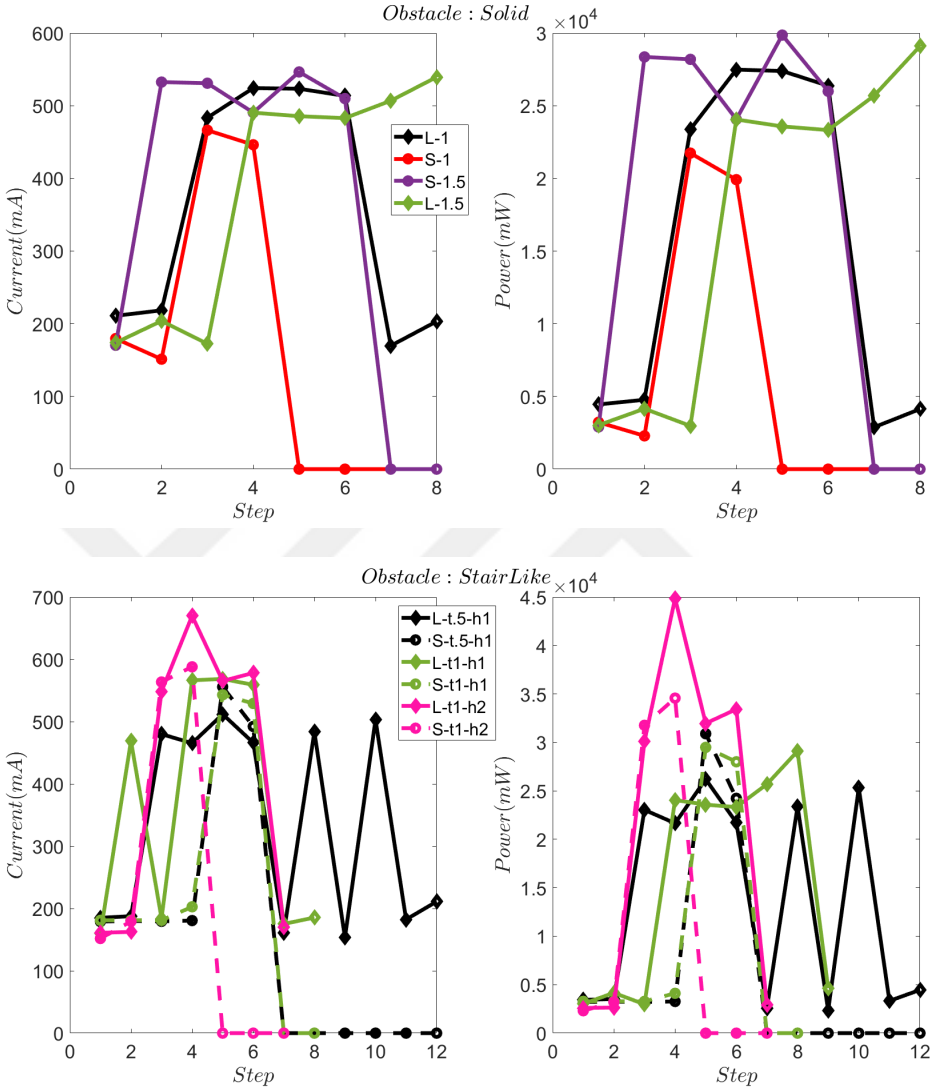

Figure 4.17: Current and power consumptions of robot during (a) Solid Obstacle Crossings. Legend express as L: long vs S: short wheel and numbers referring the obstacle heights (b) Stair-Like Obstacle Crossings. Legend express as L: long vs S: short wheel and numbers referring the obstacle instant width, t and total height, h. Mean current drawns are like following: L-t.5-h1: 332 mA, S-t.5-h1: 294 mA, L-t1-h1: 382 mA, S-t1-h1: 302 mA, L-t1-h2: 407 ma, S-t1-h2: 370 mA; hence short wheels outperform the long ones.

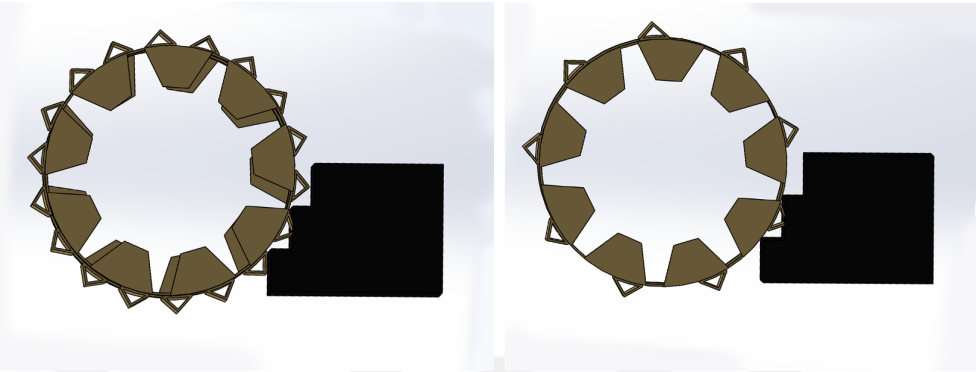

(a) (b)

Figure 4.18: Forming instant mechanical interlocking over obstacle scaling (a) on short wheel. (b) on long wheel.

4.3 Inclined Surface Climbing

This set of experiments aims to inspect the inclination rate that FAWSCY can run with long and short wheel lengths. A surface is elevated in a controlled fashion from 0° to 32° and the robot is on run with both wheel configuration. Figure 4.19 shows the experiment set-up and performance of the robot for one of the achievable angle, while Table 4.2 indicates the slope angles that the robot can perform. During the tests, for both wheel length, 26° is observed as the upper limit. Therefore, the robot can run in both wheel length configuration in case of inclined smooth surfaces. That leads us that encountering with different inclined terrains, the terrain chooses the performing wheel length rather than the slope.

Although it is indecisive which wheel length is superior by comparing physical performance, the robot's power consumption provides the wheel configuration for longer rides. Thus, on each test, the driven current and power consumption are also measured. Figure 4.20 demonstrates those measurements and it is concluded that in smaller angles, power consumption is similar, yet while angle increases, shorter wheels drive less current, thus they are more efficient to use.

Table 4.2: Achievable slope ranges on Inclined Surface Climbing for both Wheel Configurations

Wheel	Slope (°)
Short	0-26
Long	0-26

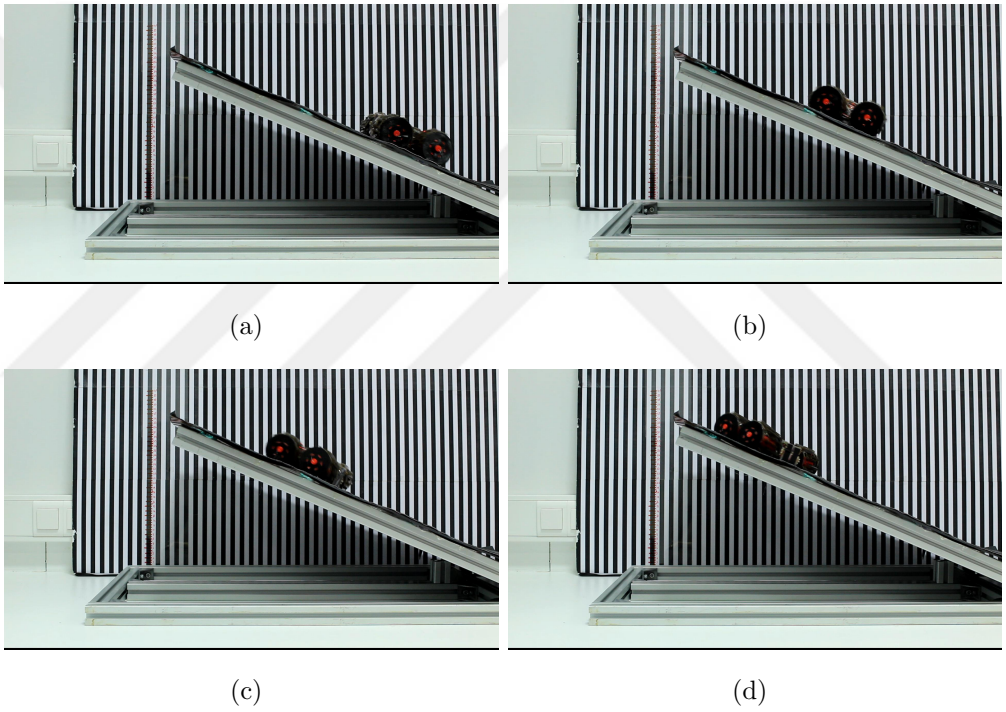

(a) (b)

(c) (d)

Figure 4.19: Test video frames to represent Inclined Surface Climbing set-up and results, when slope is 22° with closed wheels.

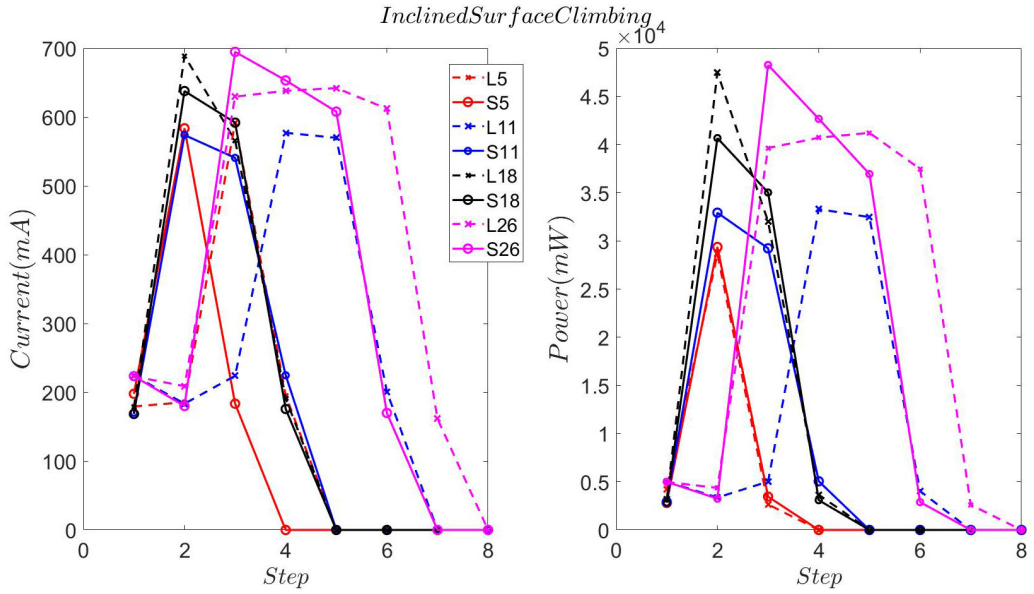

Figure 4.20: Current and power consumption of robot during inclined surface climbing. Legend express as L: long vs S: short wheel and numbers are angle of the inclination. Mean current drawns are as follows: L5: 287 mA, S5: 321 mA; L11: 329 mA, S11: 376 mA; L18: 405 mA, S18: 374 mA; L26: 444 mA; S26: 421 mA.

4.4 Fall

FAWSCY is a clumsy robot that, rather than having heavy computational sensing and controlling, its design allows it to collide with objects, drop from a certain height, encounter different mediums yet, still performs. Hence, one of the evaluations is its response to fall.

4.4.1 Modelling and Simulation

Although FAWSCY's body consists of hard materials, its wheels are mainly composed of folded PET sheets and printed flexible materials that can behave like a spring. It can bounce as a suspension system

and bend as a beam. Hence, it can absorb collision forces and minimize fracture and failure. However, FAWSCY's wheel has two separate configuration assets. Hence it also has a different response to fall. Thus, before the experiments, wheels' stiffness characteristics are evaluated. Firstly, wheels behave as a stand-alone suspension system due to its compliant design. Although, there is no passenger to assure comfort yet there exists a camera to have information about environment. Hence, to provide meaningful and processable sensing, proving ground analysis should be provided. A modified quarter car modal which is presented in Figure 4.21, is used as wheel acts as the suspension system and locomotion unit simultaneously. m is the quarter-car mass, m_t is wheel mass and K_{eff} is effective spring constant of the system. K_{eff} is measured experimentally as the design is modular, non-uniform multi-material and spare, and it is presented in Figure 4.22 for both wheel length configuration while their values are tabulated in Table 4.3.

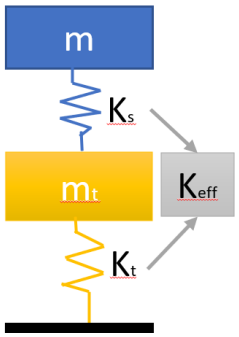

Figure 4.21: Wheel suspension system modal.

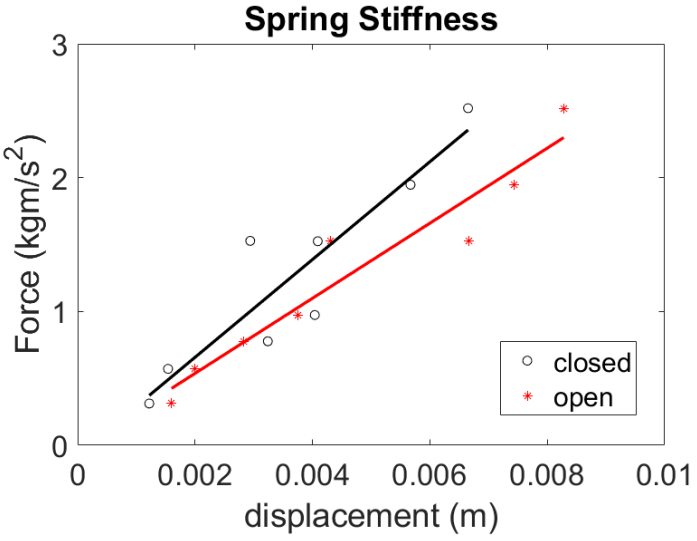

Figure 4.22: Experimental displacement vs Force values of closed and open wheels to obtain spring stiffness values tabulated in Table 4.3.

Table 4.3: Spring Stiffness Values of Wheel Configurations

Wheel	Short	Long
Stiffness (kg/s^2) : K_s	365	280

The wheel hop frequency is calculated by

$$f_{hop} = \frac{1}{2\pi}\sqrt{\frac{K_{eff}}{m}} \tag{4.1}$$

and it is tabulated in Table 4.4 for both wheel lengths. Although the wheel suspension system is analysed, the wheel cannot be differentiated from its body. Then, the hop wheel frequency analysis is more accurate [51]. By calculations, it is observed that long wheel has a lower frequency value which lays in the desired interval (10 Hz) for a comfortable ride [52] rather than the short wheel, hence it is more compliant.

Table 4.4: Natural Frequencies of Wheel Configurations

Wheel	Short	Long
Freq (Hz)	11.64	10.19

By the fall, an collision occurs that robot may jump back as if wheels are bending over the body to push against to the floor. Therefore, for both wheel configuration, a bending stiffness should be obtained. As the design is modular, non-uniform multi-material and spare, an experimental set-up is built to measure its bending stiffness and Figure 4.23 is obtained and their values are tabulated in Table 4.5.

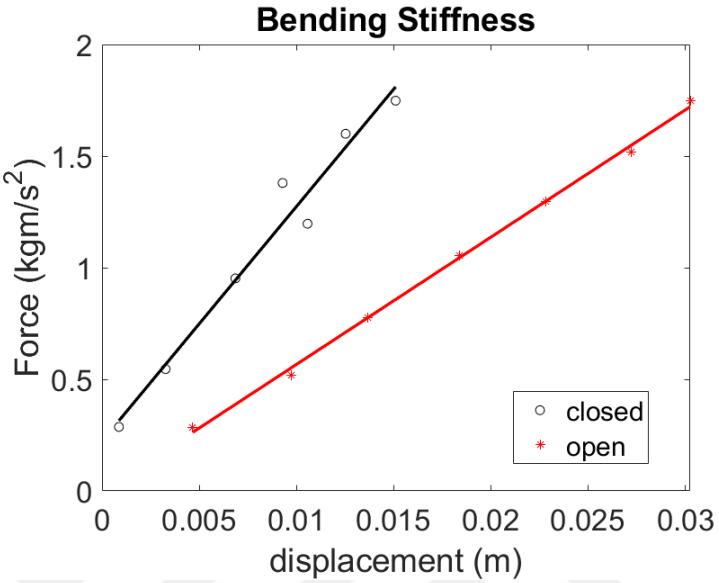

Figure 4.23: Experimental displacement vs Force values of closed and open wheels to obtain bending stiffness values tabulated in Table 4.5.

Table 4.5: Bending Stiffness Values of Wheel Configurations

Wheel	Short	Long
Stiffness (kg/s^2) : K_b	105	57

As stiffness values are available, impact force and energy on the robot can be estimated by the conservation of momentum and energy. The fall is assumed to be a free fall although robot is running, it only initiates the fall. Then, by conservation of energy, the vertical velocity of robot right before collision can be calculated by simply,

$$u = \sqrt{2gh} \tag{4.2}$$

where g is gravitational acceleration and h is the height of fall. As the robot collides with ground after free fall, its velocity drops to 0, impact force can be estimated by conservation of momentum as,

$$F = m\frac{0-u}{t_{im}} \tag{4.3}$$

being, m is the mass of robot, t_{im} is the impact duration and it is estimated as $t_{im} = 0.05$ seconds. Then, estimated impact force is coupled by stiffness to evaluate robot's vertical response to fall as,

$$z = F/K_b \tag{4.4}$$

and, fall is simulated using varied heights for the both wheel configurations. As simulation results demonstrate in Figure 4.24, open wheels are able to absorb more impact energy since it transforms the energy to higher rates of bending by having a lower stiffness.

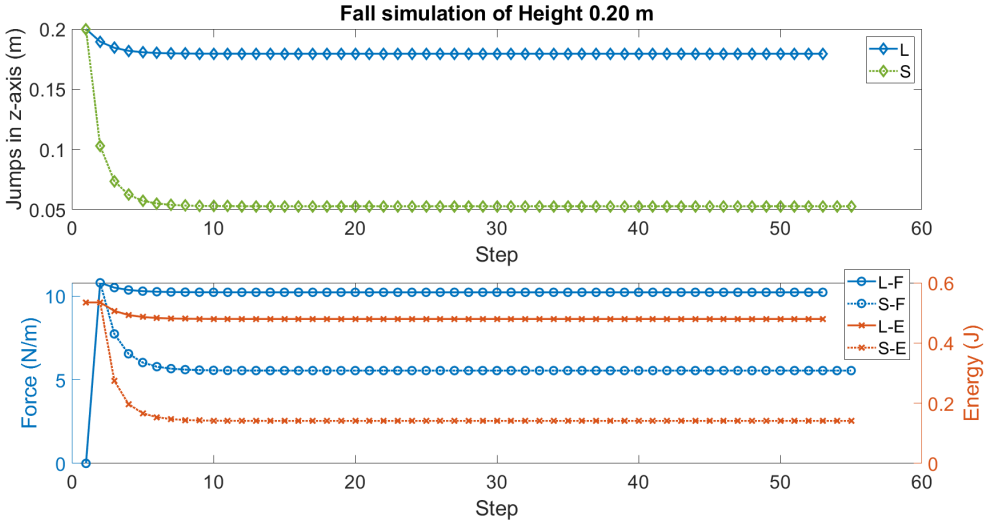

(a)

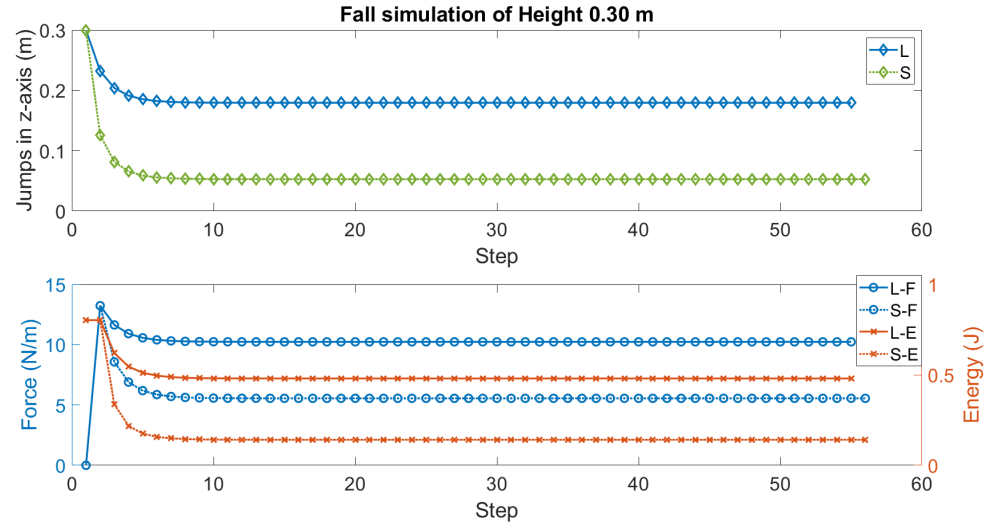

(b)

Figure 4.24: Fall impact response simulations of FAWSCY for the 20cm and 30cm heights of experiments. Simulations exhibits deflections due to fall and transmitted impact force and absorbed energy, on the first and second raws respectively. Legends are expressed as, L: long, S: short wheel and F: Impact force and E: absorbed Impact energy.

4.4.2 Experiment

Indeed, as Figure 4.25 shows, open-wheel configuration bounces yet without failure continues to its path. For both wheel configuration, fall tests are conducted till fracture is observed. The long wheel has survived all 10, 15 and 20 cm falls, yet the short wheel has failed 20 cm drop. One of the hubs is broken as it can be seen in Figure 4.26, hence the test is terminated. It can be concluded that the long wheel configurations descend the stairs in both indoor and outdoor environments since the optimum staircase rise is 17-18 mm. Yet, the open-wheel has the potential to survive from higher falls, 20 cm is not its limit.

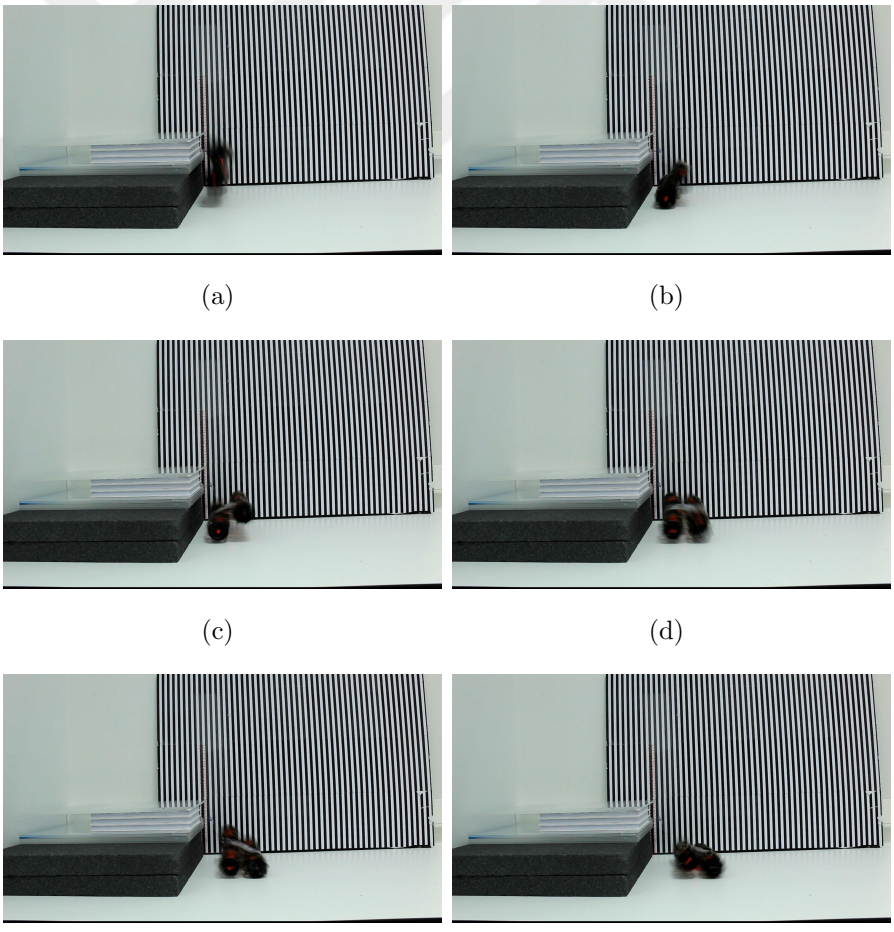

(a) (b) (c) (d) (e) (f)

Figure 4.25: Fall of open wheeled FAWSCY from 20 cm. It bounces and continues to run.

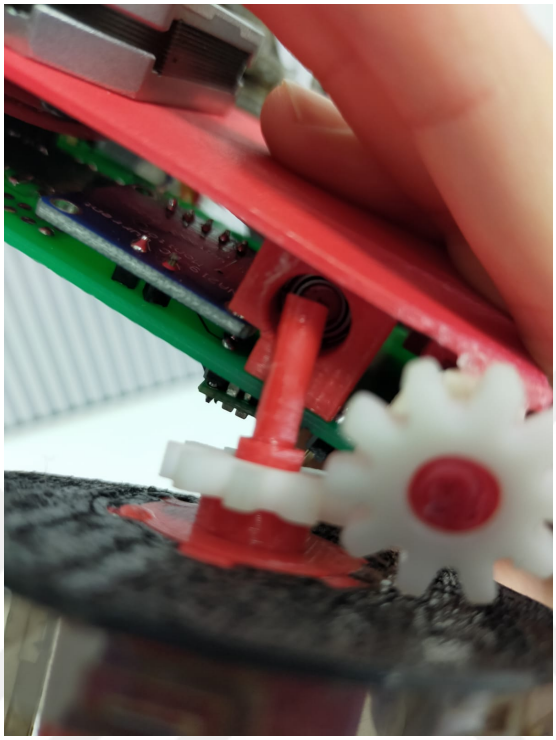

Figure 4.26: Failure of 20 cm fall with closed wheel. of As expected, failure is occurred at the shaft of hub right before bearing. At the moment of impact unabsorbed energy is transmitted through hub, resulting fail at the contact point of two tough material, PLA and steel.

4.5 Diverse Wheel Length Combinations

There are many robots in the literature that are navigated by adjustable wheel diameters, and they are also presented in Sections 1.2 and 2.2.1. Contrarily FAWSCY's wheels are adjusted by length, not by diameter, and its adjusting mechanism is already explained in detail in Section 3.2. However, an analysis is conducted to see whether the same navigation effect is observed by changing the altering parameter from diameter to length. Therefore, the robot is run without its existing control algorithm by just providing PWM to motors uthe nder the Motion Capture system, thus its position can be tracked. Figure 4.27 is formed by Motion Capture System's built-in tracking camera in MJPEG mode to

demonstrate test area and conditions. Its reference coordinate is also indicated. The robot runs along the x-axis in the range of $[0.3 - 1.5]$ m, and the divergence along the y-axis indicates if it navigates towards left or right.

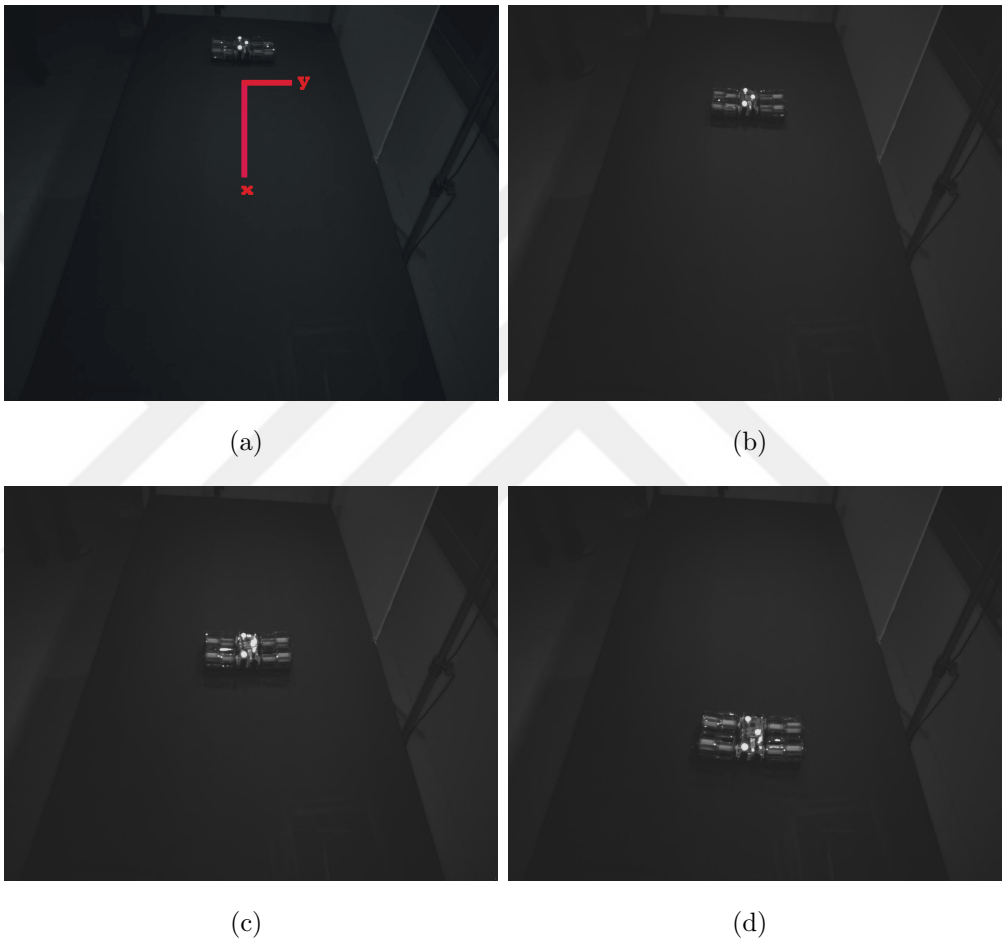

(a) (b)

(c) (d)

Figure 4.27: Test video frames to represent Motion Capture system, with open wheels.

First of all, changes on-axis are presented in Figure 4.28. As it proceeds along the x-axis, gear pairs on wheels cannot position identically, and a constant height cannot be maintained. It oscillates in an interval of $[55 - 57]mm$ along the z-axis. It can also drift on the y-axis due to disturbances and that dissimilar gear positioning. Initially, symmetric runs are conducted, i.e., when all wheels or only diagonals are in short or long-form. Those trackings are presented in Figure 4.29. Although the robot seems to intent going on the left side overall, it oscillates

along the y-axis, and oscillations do not exceed its body length along the y-axis, which is 57 mm. In Figure 4.30, FAWSCY runs when only one side (left or right) of its wheels is open and the open side is changing by runs. It is observed that closed-form drifts more. On the other hand, as Figure 4.31 indicates, when one of the wheels are in a different configuration than others, it tends to drift that side.

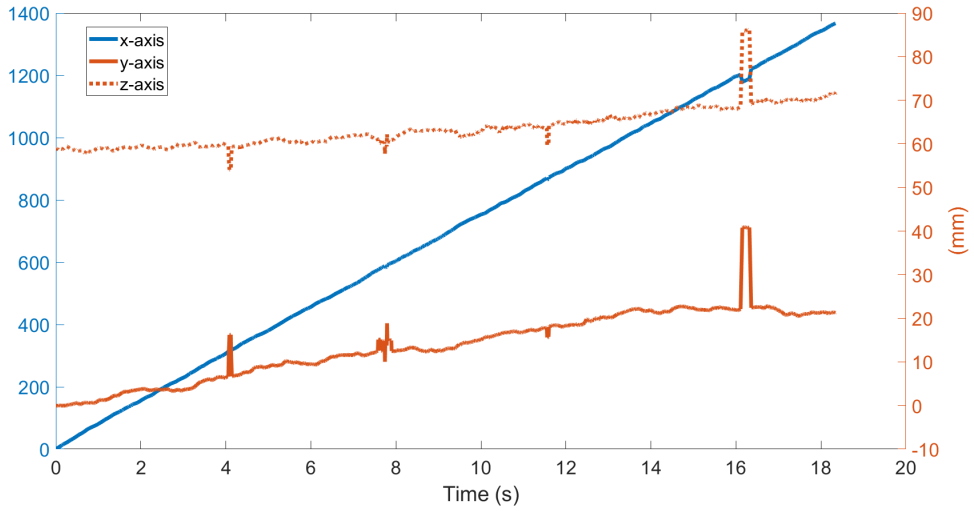

Figure 4.28: Divergences on axes while FAWSCY runs

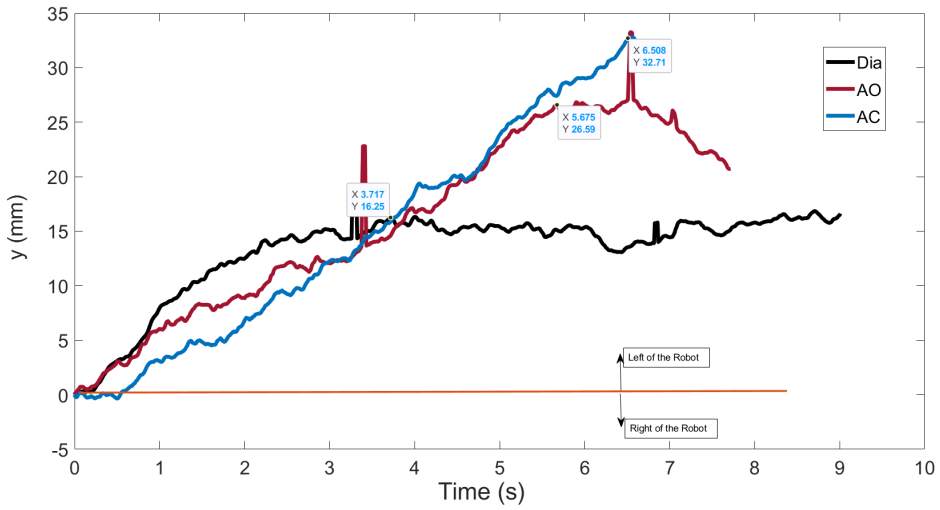

Figure 4.29: Divergence along y-axis when running uncontrolled fashion along x-axis with symmetric wheel configurations. Label represents Dia: diagonal wheels are either open or closed, AO: all open and AC: all closed.

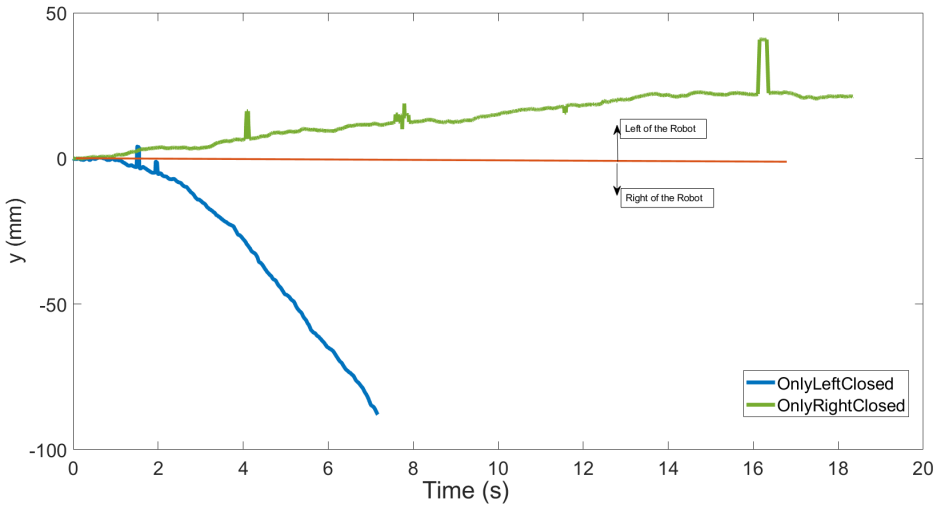

Figure 4.30: Divergence along y-axis when running uncontrolled fashion along x-axis with only left or right wheels of robot are closed configuration.

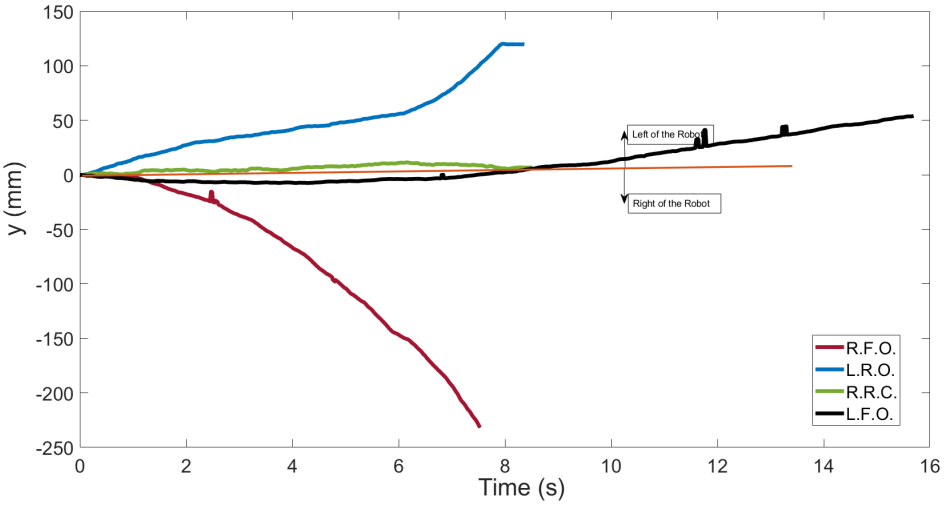

Figure 4.31: Divergence along y-axis when running uncontrolled fashion along x-axis with only one of four wheels have different configuration than others. Label formed as first letter being R: right, L: left; second letter being F: front, R: rear; and last letter being O: open, C: closed.

4.6 Discussion on The Results

Experiments verified that FAWSCY is a collision resilient, rough terrain robot to attain SAR missions and somatic activities. It is demonstrated that it can absorb unexpected forces, i.e., collisions with human beings and animals, and continue its run. It steers along forward and reverse direction with turns. It also turns around itself in a point.

Through the rough terrain experiments, it is observed that it can successfully run on various environments such as concrete indoor-outdoor terrains, grass, gravels, and soil. On grass terrain, the long wheel is superior to the short one, while on other terrains, either the short wheel outperforms or the performance of short and long wheels are indifferent. The power consumption of the robot during runs also reflects the performance of runs. If a wheel length struggles to run on the terrain, it also consumes more power to overcome the terrain.

During the obstacle scaling experiments, FAWSCY exhibited significantly higher performance with short wheels as they increase the interlock between objects and exert more traction force. Indeed, its power consumption rates also promote that the short wheel consumes less energy to go over an obstacle while long ones dissipate the energy on the struggle.

FAWSCY can also climb over inclined surfaces up to 26° of inclination in both wheel length configuration. Yet, its power consumption rates indicate that long wheels are more efficient in lower rates of inclinations, while in higher rates, short ones are.

Measurements and simulations on FAWSCY's wheel configurations shown that long wheel configuration has lower bending and spring stiffness' which means it can deform elastically more than short ones. Hence, long wheels provide a more comfortable ride for the camera and absorb more impact energy and fall from higher heights without being damaged. Indeed, during the fall experiments, short wheeled robot failed to fall from 20 cm, and its shaft was broken, while the long wheel configuration fell and continued its motion after falling 20 cm of height. Higher height experiments have not been conducted. Thus, it is not determined the height that long wheeled robot would fail.

Chapter 5

Conclusion and Future Work

By FAWSCY, it is desired to build a robot that exhibits excessive manoeuvrer capabilities and collision resilient characteristics. In order to achieve those characteristics, various wheel and body combinations are attempted, and it is settled into the final version. By the help of its foldable, lightweight and flexible design, it attains untethered and long-duration runs under various navigation commands. It is able to maintain its run after crashes and falls without being harmed or harming collided objects while climbing over inclinations and encountered half-sized obstacles compared to its body height. Additionally, it would run on diversely featured terrains. Analysis of FAWSCY is comprehensively discussed in Chapter 4, it is observed that research aims of this work are acquired.

On the other hand, experiments not only validates FAWSCY's features but also light the insight of enhancements and developments. One of the improvements can be PDMS coating. As Section 2.2.4.3 presents, PDMS coating on wheels improves traction forces, hence increases achievable inclination rate and obstacle height. Another cultivation may be focused on body and gear-set positioning. Mainly on various terrain experiments (Section 4.1.4), and also in other tests, it is observed that any penetration from the body itself or external to gear-set interrupts the motion transmission on this gear set. Thus, the wheel malfunctions and drifts the robot towards its direction.

The final version of FAWSCY presents fully-functional runs by communication of the motherboard and the drive unit. However, the motherboard, consisted of Raspberry Pi and Pi Camera, is not used in its full capacity. A higher-level control architecture can be built such that data extracted from the camera, real-time videos or stored images, is processed to provide navigation commands. Therefore, the need for a operator during the tasks can be eliminated and FAWSCY becomes fully automated.

Further development on FAWSCY can be individually adjusted wheel lengths. By the initial analysis presented in Section 4.5 already demonstrates that the different wheel length combinations result in different steering. Further evaluations may lead to higher performance of steering than currently available steering policy, or varied adjustments on length may improve the manoeuvre capability on diverse terrains or maze-like narrow trajectories.

Bibliography

[1] A. F. Güç, M. A. I. Kalin, C. Karakadioğlu, and O. Özcan, "C-Quad: A miniature, foldable quadruped with C-shaped compliant legs," *2017 IEEE International Conference on Robotics and Biomimetics, ROBIO 2017*, vol. 2018-Janua, pp. 1–6, 2018.

[2] E. Shimada, J. Thompson, J. Yan, R. Wood, and R. Fearing, "Prototyping millirobots using dextrous microassembly and folding," *Symposium on Microrobotics ASME Int. Mechanical Engineering Cong. and Exp*, pp. 1–8, 2000.

[3] R. J. Wood, S. Avadhanula, R. Sahai, E. Steltz, and R. S. Fearing, "Microrobot design using fiber reinforced composites," *Journal of Mechanical Design, Transactions of the ASME*, vol. 130, no. 5, 2008.

[4] A. M. Hoover, E. Steltz, and R. S. Fearing, "RoACH: An autonomous 2.4g crawling hexapod robot," *2008 IEEE/RSJ International Conference on Intelligent Robots and Systems, IROS*, pp. 26–33, 2008.

[5] P. Birkmeyer, K. Peterson, and R. S. Fearing, "DASH: A dynamic 16g hexapedal robot," *2009 IEEE/RSJ International Conference on Intelligent Robots and Systems, IROS 2009*, pp. 2683–2689, 2009.

[6] S. Felton, M. Tolley, E. Demaine, D. Rus, and R. Wood, "A method for building self-folding machines," *Science*, vol. 345, no. 6197, pp. 644–646, 2014.

[7] J. Rossiter and S. Sareh, "Kirigami design and fabrication for biomimetic robotics," *Bioinspiration, Biomimetics, and Bioreplication 2014*, vol. 9055, p. 90550G, 2014.

[8] A. M. Mehta and D. Rus, "An end-to-end system for designing mechanical structures for print-and-fold robots," *Proceedings - IEEE International Conference on Robotics and Automation*, pp. 1460–1465, 2014.

[9] C. D. Onal, R. J. Wood, and D. Rus, "Towards printable robotics: Origami-inspired planar fabrication of three-dimensional mechanisms," *Proceedings - IEEE International Conference on Robotics and Automation*, pp. 4608–4613, 2011.

[10] C. Karakadioğlu, M. Askari, and O. Özcan, "Design and operation of MinIAQ: An untethered foldable miniature quadruped with individually actuated legs," *IEEE/ASME International Conference on Advanced Intelligent Mechatronics, AIM*, pp. 247–252, 2017.

[11] M. Askari, C. Karakadioğlu, F. Ayhan, and O. Özcan, "MinIAQ-II: A miniature foldable quadruped with an improved leg mechanism," *2017 IEEE International Conference on Robotics and Biomimetics, ROBIO 2017*, vol. 2018-Janua, pp. 1–7, 2018.

[12] N. Mahkam, A. Bakir, and O. Ozcan, "Miniature Modular Legged Robot with Compliant Backbones," *IEEE Robotics and Automation Letters*, vol. 5, no. 3, pp. 3923–3930, 2020.

[13] C. D. Onal, M. T. Tolley, R. J. Wood, and D. Rus, "Origami-Inspired Printed Robots," *IEEE/ASME Transactions on Mechatronics*, vol. 20, no. 5, pp. 2214–2221, 2015.

[14] J. E. Rajkowski, A. P. Gerratt, E. W. Schaler, and S. Bergbreiter, "A Multi-Material Milli-Robot Prototyping Process," pp. 2777–2782, 2009.

[15] J. P. Whitney, P. S. Sreetharan, K. Y. Ma, and R. J. Wood, "Pop-up book MEMS," *Journal of Micromechanics and Microengineering*, vol. 21, no. 11, 2011.

[16] O. Ozcan, A. T. Baisch, and R. J. Wood, "Design and feedback control of a biologically-inspired miniature quadruped," *IEEE International Conference on Intelligent Robots and Systems*, pp. 1438–1444, 2013.

[17] M. Karpelson, B. H. Waters, B. Goldberg, B. Mahoney, O. Ozcan, A. Baisch, P. M. Meyitang, J. R. Smith, and R. J. Wood, "A wirelessly powered, biologically inspired ambulatory microrobot," *Proceedings - IEEE International Conference on Robotics and Automation*, pp. 2384–2391, 2014.

[18] Y. Mulgaonkar, B. Araki, J. S. Koh, L. Guerrero-Bonilla, D. M. Aukes, A. Makineni, M. T. Tolley, D. Rus, R. J. Wood, and V. Kumar, "The flying monkey: A mesoscale robot that can run, fly, and grasp," *Proceedings - IEEE International Conference on Robotics and Automation*, vol. 2016-June, pp. 4672–4679, 2016.

[19] R. Maccurdy, R. Katzschmann, Y. Kim, and D. Rus, "Printable hydraulics: A method for fabricating robots by 3D co-printing solids and liquids," *Proceedings - IEEE International Conference on Robotics and Automation*, vol. 2016-June, pp. 3878–3885, 2016.

[20] E. B. Joyee and Y. Pan, "Multi-material additive manufacturing of functional soft robot," *Procedia Manufacturing*, vol. 34, pp. 566–573, 2019.

[21] M. A. I. Kaln, C. Aygul, A. Turkmen, J. Kwiczak-Yigitbas, B. Baytekin, and O. Ozcan, "Design, Fabrication, and Locomotion Analysis of an Untethered Miniature Soft Quadruped, SQuad," *IEEE Robotics and Automation Letters*, vol. 5, no. 3, pp. 3854–3860, 2020.

[22] Y. Sun, S. Song, X. Liang, and H. Ren, "A Miniature Soft Robotic Manipulator Based on Novel Fabrication Methods," *IEEE Robotics and Automation Letters*, vol. 1, no. 2, pp. 617–623, 2016.

[23] M. R. Cutkosky and S. Kim, "Design and fabrication of multi-material structures for bioinspired robots," *Philosophical Transactions of the Royal Society A: Mathematical, Physical and Engineering Sciences*, vol. 367, no. 1894, pp. 1799–1813, 2009.

[24] A. Bruyas, F. Geiskopf, and P. Renaud, "Toward unibody robotic structures with integrated functions using multimaterial additive manufacturing: Case study of an MRI-compatible interventional device," *IEEE International Conference on Intelligent Robots and Systems*, vol. 2015-Decem, pp. 1744–1750, 2015.

[25] U. Saranli, M. Buehler, and D. E. Koditschek, "RHex: A Simple and Highly Mobile Robot," *International Journal of Robotics Research*, vol. 20, no. 7, pp. 616–631, 2001.

[26] H. Gao, S. Bi, R. Zhang, and S. Tang, "The design of a throwable two-wheeled reconnaissance robot," *2012 IEEE International Conference on Robotics and Biomimetics, ROBIO 2012 - Conference Digest*, pp. 2150–2155, 2012.

[27] R. Lang, *The Complete Book of Origami: Step-by-Step Instructions in Over 1000 Diagrams*. New York: Dover Publications, Inc., 1988.

[28] "Dupont™ kapton® hn." online.

[29] T. Y. Kim, C. Kim, S. H. Kim, and G. P. Jung, "MutBug: A lightweight and compact crawling robot that can run on both sides," *IEEE Robotics and Automation Letters*, vol. 4, no. 2, pp. 1409–1415, 2019.

[30] S. C. Chen, K. J. Huang, W. H. Chen, S. Y. Shen, C. H. Li, and P. C. Lin, "Quattroped: A leg-wheel transformable robot," *IEEE/ASME Transactions on Mechatronics*, vol. 19, no. 2, pp. 730–742, 2014.

[31] K. Nagatani, M. Kuze, and K. Yoshida, "Development of a Transformable Mobile Robot with a Variable Wheel Diameter," *Journal of Robotics and Mechatronics*, vol. 19, no. 3, pp. 252–257, 2007.

[32] D. Y. Lee, J. S. Kim, S. R. Kim, J. S. Koh, and K. J. Cho, "The deformable wheel robot using magic-ball origami structure," *Proceedings of the ASME Design Engineering Technical Conference*, vol. 6 B, pp. 1–9, 2013.

[33] D. Y. Lee, J. S. Koh, J. S. Kim, S. W. Kim, and K. J. Cho, "Deformable-wheel robot based on soft material," *International Journal of Precision Engineering and Manufacturing*, vol. 14, no. 8, pp. 1439–1445, 2013.

[34] D. Y. Lee, G. P. Jung, M. K. Sin, S. H. Ahn, and K. J. Cho, "Deformable wheel robot based on origami structure," *Proceedings - IEEE International Conference on Robotics and Automation*, pp. 5612–5617, 2013.

[35] S. M. Felton, D. Y. Lee, K. J. Cho, and R. J. Wood, "A passive, origami-inspired, continuously variable transmission," *Proceedings - IEEE International Conference on Robotics and Automation*, pp. 2913–2918, 2014.

[36] B. P. Rhoads and H. J. Su, "The design and fabrication of a deformable origami wheel," *Proceedings of the ASME Design Engineering Technical Conference*, vol. 5B-2016, no. August, 2016.

[37] H. Kimura and S. Hirose, "Development of Genbu: Active wheel passive joint articulated mobile robot," *IEEE International Conference on Intelligent Robots and Systems*, vol. 1, no. October, pp. 823–828, 2002.

[38] S. Shrivastava, A. Karsai, Y. O. Aydin, R. Pettinger, W. Bluethmann, R. O. Ambrose, and D. I. Goldman, "Material remodeling and unconventional gaits facilitate locomotion of a robophysical rover over granular terrain," *Science Robotics*, vol. 5, no. 42, pp. 1–11, 2020.

[39] P. Abad-Manterola, J. W. Burdick, I. A. Nesnas, S. Chinchali, C. Fuller, and X. Zhou, "Axel rover paddle wheel design, efficiency, and sinkage on deformable terrain," *Proceedings - IEEE International Conference on Robotics and Automation*, pp. 2821–2827, 2010.

[40] D. Y. Lee, S. R. Kim, J. S. Kim, J. J. Park, and K. J. Cho, "Origami wheel transformer: A variable-diameter wheel drive robot using an origami structure," *Soft Robotics*, vol. 4, no. 2, pp. 163–180, 2017.

[41] "How to make 8 pointed transforming ninja star – step by step origami tutorial," Sept. 2020.

[42] E. Vander Hoff, D. Jeong, and K. Lee, "OrigamiBot-I: A thread-actuated origami robot for manipulation and locomotion," *IEEE International Conference on Intelligent Robots and Systems*, no. Iros, pp. 1421–1426, 2014.

[43] J. Butler, N. Pehrson, T. Bateman, J. Morgan, and L. L. Howell, "DETC2016-59060," pp. 1–11, 2016.

[44] J. Butler, S. Magleby, L. Howell, S. Mancini, and A. Parness, "Highly compressible origami bellows for microgravity drilling-debris containment," *AIAA SPACE and Astronautics Forum and Exposition, SPACE 2017*, no. 203999, pp. 1–16, 2017.

[45] N. Kidambi and K. W. Wang, "On the deployment of multistable kresling origami-inspired structures," *Proceedings of the ASME Design Engineering Technical Conference*, vol. 5B-2019, pp. 1–10, 2019.

[46] H. In, B. B. Kang, M. K. Sin, and K. J. Cho, "Exo-Glove: A wearable robot for the hand with a soft tendon routing system," *IEEE Robotics and Automation Magazine*, vol. 22, no. 1, pp. 97–105, 2015.

[47] U. Jeong, H. In, H. Lee, B. B. Kang, and K. J. Cho, "Investigation on the control strategy of soft wearable robotic hand with slack enabling tendon actuator," *Proceedings - IEEE International Conference on Robotics and Automation*, vol. 2015-June, no. June, pp. 5004–5009, 2015.

[48] M. Abbasi and S. A. A. Moosavian, "RoboGlove: Design of a Tendon-Driven Robotic Glove with Differential Mechanisms," *ICRoM 2019 - 7th International Conference on Robotics and Mechatronics*, no. ICRoM, pp. 480–486, 2019.

[49] J. Zhao, W. Yan, N. Xi, M. W. Mutka, and L. Xiao, "A miniature 25 grams running and jumping robot," *Proceedings - IEEE International Conference on Robotics and Automation*, pp. 5115–5120, 2014.

[50] Texas Insturments, *Zerø-Drift, Bi-DirectionalCURRENT/POWER MONITOR with I2C™ Interface*, Aug. 2008.

[51] T. M. Allred, "Compliant Mechanism Suspensions," *Department of Mechanical Engineering*, vol. MsC, no. August, p. 159, 2003.

[52] P. Barak, "SA E TECHNICAL Magic Numbers in Design of Suspensions for Passenger Cars," 2018.